

Out-of-Distribution Knowledge Distillation via Confidence Amendment

Zhilin Zhao^{1*}, Longbing Cao¹ and Yixuan Zhang²

¹Data Science Lab, School of Computing and DataX Research Centre, Macquarie University, Sydney, 2109, NSW, Australia.

²China-Austria Belt and Road Joint Laboratory on Artificial Intelligence and Advanced Manufacturing, Hangzhou Dianzi University, Hangzhou, 310005, Zhejiang, China.

*Corresponding author(s). E-mail(s): zhaozh17@hotmail.com;

Contributing authors: longbing.cao@mq.edu.au; yixuan.zhang@hdu.edu.cn;

Abstract

Out-of-distribution (OOD) detection is essential in identifying test samples that deviate from the in-distribution (ID) data upon which a standard network is trained, ensuring network robustness and reliability. This paper introduces OOD knowledge distillation, a pioneering learning framework applicable whether or not training ID data is available, given a standard network. This framework harnesses OOD-sensitive knowledge from the standard network to craft a binary classifier adept at distinguishing between ID and OOD samples. To accomplish this, we introduce Confidence Amendment (CA), an innovative methodology that transforms an OOD sample into an ID one while progressively amending prediction confidence derived from the standard network. This approach enables the simultaneous synthesis of both ID and OOD samples, each accompanied by an adjusted prediction confidence, thereby facilitating the training of a binary classifier sensitive to OOD. Theoretical analysis provides bounds on the generalization error of the binary classifier, demonstrating the pivotal role of confidence amendment in enhancing OOD sensitivity. Extensive experiments spanning various datasets and network architectures confirm the efficacy of the proposed method in detecting OOD samples.

Keywords: Deep Neural Networks, Out-of-distribution Detection, Knowledge Distillation, Generalization Error Bound

1 Introduction

Deep neural networks trained on *in-distribution* (ID) samples have demonstrated remarkable generalization capabilities for test samples that align with the same distribution [Suzuki, Abe, and Nishimura \(2020\)](#). However, they struggle when encountering *out-of-distribution* (OOD) samples derived from different distributions [J. Yang et](#)

[al. \(2022\)](#); [Zhao, Cao, and Lin \(2023a\)](#). Alarmingly, these networks are prone to assigning high-confidence predictions to such OOD samples, thereby blurring the critical distinction between ID and OOD samples [Zhao, Cao, and Lin \(2023c\)](#). This issue arises because standard training procedures do not impose constraints on how the network should react to OOD samples, resulting in distribution vulnerability [Zhao, Cao, and Lin \(2023b\)](#). In real-world applications, the inability

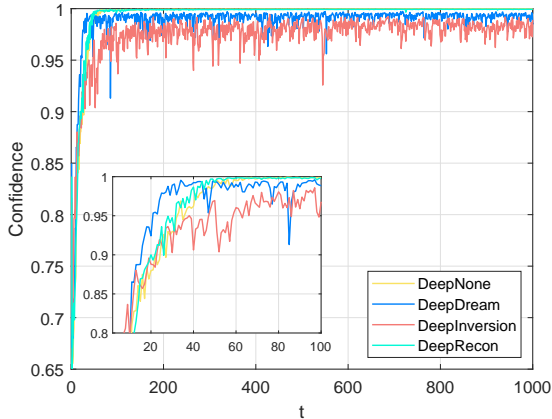


Fig. 1 Variations in confidence levels for synthesized images over iterations using different methods. The standard network, built on a ResNet18 backbone, is trained on the CIFAR10 dataset. DeepNone amplifies the confidence of noise by optimizing for cross-entropy loss using a random label, without any regularization constraints. In contrast, both DeepDream [Mordvintsev, Olah, and Tyka \(2015\)](#) and DeepInversion [Yin et al. \(2020\)](#) apply additional regularizations to the synthesized samples. When original ID data is available, DeepRecon employs mean squared error to enhance confidence by more closely approximating the original ID data. Best viewed in color.

to identify OOD samples can lead to severe consequences, emphasizing the critical importance of OOD detection.

For a standard network trained on ID samples, existing methodologies for detecting its OOD samples fall into two main categories [Salehi et al. \(2022\)](#). The first relies on post-hoc analysis of the output from networks, without altering the original architecture or needing access to the original ID training data. These methods, however, are intrinsically limited by the sensitivity of the existing network to OOD samples. The second modifies the loss function and training process by incorporating OOD prior knowledge. While this enhances OOD sensitivity, it compromises the generalization capabilities for ID samples and necessitates retraining networks on the original ID training data, which can be impractical due to data privacy and security concerns.

To integrate the advantages of these two existing algorithms and address their shortcomings, we propose a new learning framework called *OOD Knowledge Distillation*. This framework extracts OOD-sensitive knowledge from a standard network and transfers it to a binary classifier tailored for discerning between ID and OOD samples. The primary challenge lies in gleaning meaningful

knowledge from the standard network, particularly in the absence of the original ID training data, and refining this knowledge to enhance OOD sensitivity. This process requires synthesizing network-specific ID and OOD samples to extract knowledge that is acutely sensitive to OOD samples. Moreover, the extracted knowledge should not merely be transferred and also needs to be aligned with prior OOD insights to further amplify OOD sensitivity.

Inspired by adversarial sample generation [Goodfellow, Shlens, and Szegedy \(2015\)](#) and diffusion probabilistic models [Ho, Jain, and Abbeel \(2020\)](#); [Sohl-Dickstein, Weiss, Maheswaranathan, and Ganguli \(2015\)](#), a random noise can progress toward an ID sample by incrementally applying subtle perturbations in each transition, enabling the simultaneous synthesis of both ID and OOD samples. These perturbations, anchored in the traditional cross entropy loss and a sample constraint, enhance its confidence at each step. The sample constraint guides the synthesis of samples by involving prior knowledge about ID samples in the scenario where training ID samples are unavailable [Mordvintsev et al. \(2015\)](#); [Yin et al. \(2020\)](#). Conversely, when training ID samples are available, it aligns the synthesized samples with their distribution [Kingma and Welling \(2014\)](#). Random noise is viewed as an OOD sample because it follows a distribution different from the training ID. However, an OOD sample with only a few transitions remains OOD, but might exhibit an unexpectedly high-confidence prediction, as illustrated in Fig. 1. This implies that it is imprudent to fully trust the confidence from the standard network and necessary to encourage the samples in the early stage of the transition to their own low-confidence predictions.

Confidence Amendment (CA) is introduced to tackle the challenges associated with OOD knowledge distillation. It aims to train a specialized binary classifier for a standard network, with the primary goal of distinguishing between ID and OOD samples. Based on the observations from the synthesis of ID and OOD samples, CA progressively converts an OOD sample into an ID sample for synthesis, while concurrently enhancing reliance on confidence, thus promoting lower confidence for OOD samples. Accordingly, CA employs a parameterized Markov chain [Duan, Wang, Wen,](#)

and Yuan (2020) to convert random noise into a high-confidence ID sample, synthesizing a sample at each transition. The predicted label distributions from the standard network of these synthesized samples are integrated with a Uniform distribution. Notably, early and later stages of the synthesized samples within this Markov chain carry higher and lower weights on these distributions, respectively. Ultimately, these synthesized samples, with their adjusted predicted label distributions, are utilized to train a binary classifier. This classifier is tailored to discern between samples of high and low confidence levels, thereby equipping it to differentiate between ID and OOD samples.

The main contributions of this paper include:

- The inception of a groundbreaking learning framework dubbed OOD knowledge distillation, crafted to distill OOD-sensitive knowledge from a standard network, culminating in a binary classifier tuned to distinguish between ID and OOD samples.
- In the development of this binary classifier, Confidence Amendment (CA) gradually transforms an OOD sample into an ID sample while progressively placing trust in the prediction confidence.
- The generalization error bound of the binary classifier demonstrates that refining the knowledge derived from the standard network significantly bolsters its capability to differentiate between ID and OOD samples. Comprehensive experimental results validate the efficacy of the method.

The rest of this paper is organized as follows: Section 2 offers an overview of related techniques and research directions. Section 4 elaborates on the proposed Confidence Amendment (CA) method. Section 5 and Section 6 present the theoretical guarantees and empirical results, respectively. Finally, Section 7 provides concluding remarks and discusses future directions.

2 Related Work

In this section, we introduce OOD detection, knowledge distillation, data-free distillation, and data synthesis.

2.1 Out-of-distribution Detection

For a network trained on ID data, OOD detection Salehi et al. (2022); J. Yang, Zhou, Li, and Liu (2021); J. Yang, Zhou, and Liu (2023) aims to identify samples that deviate from the distribution of the ID ones. Current methods primarily fall into two groups: those that refrain from using training ID data Ahn, Park, and Kim (2023); Gomes, Alberge, Duhamel, and Piantanida (2022); Hendrycks et al. (2022); Lee, Lee, Lee, and Shin (2018a); Olber, Radlak, Popowicz, Szczepankiewicz, and Chachula (2023); Sun, Guo, and Li (2021); J. Zhang et al. (2023); J. Zhu et al. (2023); Y. Zhu et al. (2022) and those that incorporate it Bibas, Feder, and Hasnner (2021); Cao and Zhang (2022); Dong et al. (2022); Hein, Andriushchenko, and Bitterwolf (2019); Hsu, Shen, Jin, and Kira (2020); Zhao et al. (2023b).

2.1.1 Methods Not Utilizing Training ID Data

OOD detection methods that do not use training ID data compute an OOD score based on the outputs of a trained network, without altering the training process or objective. Maximum over Softmax Probability (MSP) Hendrycks and Gimpel (2017) uses the maximum probabilities from softmax distributions to detect OOD samples, as correctly classified examples usually exhibit higher maximum softmax probabilities compared to OOD samples. Energy-Based Detector (EBD) W. Liu, Wang, Owens, and Li (2020) introduces an energy score for OOD detection, which is more aligned with the probability density of inputs and less prone to overconfidence issues compared to traditional softmax confidence scores. GradNorm R. Huang, Geng, and Li (2021) detects OOD inputs by leveraging information from the gradient space, specifically utilizing the vector norm of gradients derived from the KL divergence between the softmax output and a uniform probability distribution. GEN X. Liu, Lochman, and Zach (2023) introduces a generalized entropy score function, suitable for any pre-trained softmax-based classifier. Decoupling MaxLogit (DML) Z. Zhang and Xiang (2023) is an advanced logit-based OOD detection method that decouples MaxCosine and MaxNorm from standard logits to enhance OOD detection.

ASH Djuricic, Bozanic, Ashok, and Liu (2023) is a post-hoc, on-the-fly activation shaping method for OOD detection that removes a significant portion of a late-layer activation during inference without requiring statistics from training data. FeatureNorm Yu, Shin, Lee, Jun, and Lee (2023) computes the norm of the feature map from a selected block, rather than the last one, and utilizes jigsaw puzzles as pseudo OOD to select the optimal block. These methods predominantly hinge on the insights gleaned from trained networks, constraining the potential for elevating OOD sensitivity. On the other hand, OOD knowledge distillation garners OOD-sensitive knowledge by synthesizing samples for a trained network, unveiling its distribution vulnerabilities and bolstering its sensitivity to OOD.

2.1.2 Methods Utilizing Training ID Data

OOD detection methods that use training ID data improve the OOD sensitivity of a trained network by either maintaining or fine-tuning it with training ID data, incorporating OOD prior knowledge. Confidence-Calibrated Classifier (CCC) Lee, Lee, Lee, and Shin (2018b) incorporates two additional terms into the traditional cross entropy loss: one that reduces confidence in OOD samples and another for implicitly generating beneficial training samples, simultaneously training classification and generative networks for OOD detection. Minimum Others Score (MOS) R. Huang and Li (2021) segments the semantic space into smaller groups of analogous concepts, streamlining decision boundaries for efficient OOD detection. Density-Driven Regularization (DDR) W. Huang, Wang, Xia, Wang, and Zhang (2022) introduces two constraints: a density consistency regularization aligning analytical and empirical label densities, and a contrastive distribution regularization distinguishing ID from OOD samples. Watermarking Wang et al. (2022) taps into the reprogramming capacity of deep models, integrating a distinct feature perturbation to data, boosting OOD detection without altering model parameters. CIDER Ming, Sun, Dia, and Li (2023) employs hyperspherical embeddings and optimizes both a dispersion loss ensuring vast angular distances between class prototypes and a compactness loss, making certain samples remain proximate to their

class prototypes. HEAT Lafon, Ramzi, Rambour, and Thome (2023) offers an energy-based rectification of a blend of class-conditional Gaussian distributions to address OOD detection, remedying the MCMC sampling non-mixing issue during the training of energy-based models. Dual Representation Learning (DRL) Zhao and Cao (2023) harnesses both robust and subtle label-associated information, instructing an auxiliary network to discern distribution-discriminative representations that complement the label-discriminative insights of a pre-existing network, thereby enhancing OOD detection performance. Despite their pioneering methods, these OOD algorithms frequently necessitate extra training phases for retraining or fine-tuning pre-existing networks, which can compromise generalization capabilities and make their integration and scalability more challenging in real-world scenarios. In contrast, OOD knowledge distillation extracts knowledge from a trained network to develop its OOD-sensitive binary classifier without altering the network itself.

2.2 Knowledge and Data-free Distillation

Knowledge distillation Allen-Zhu and Li (2023); Gou, Yu, Maybank, and Tao (2021) refers to the process wherein a smaller model is trained to mimic the behavior of a larger, more complex model. One of the seminal works in this area is by Hinton et al. Hinton, Vinyals, and Dean (2015), in which they introduced the idea of using the soft outputs of the teacher model to train the student. Following this, FitNets Romero et al. (2015) leverages intermediate representations from the teacher to guide the student model. Lopez-Paz et al. Lopez-Paz, Bottou, Schölkopf, and Vapnik (2016) present a unified perspective on knowledge distillation, showing its relation to privileged information. Traditional knowledge distillation requires access to the original training dataset. However, in some scenarios, this data might not be accessible due to storage constraints, privacy concerns, or other logistical issues. To address this challenge, data-free distillation has emerged, which aims to transfer knowledge from a teacher model to a student model without access to the original training data. Chen et al. Chen et al. (2019) use data-free learning where synthetic

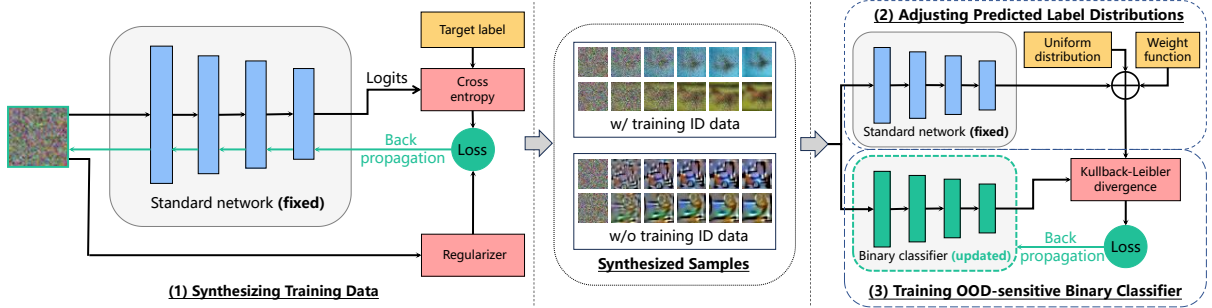


Fig. 2 Overview of the Confidence Amendment (CA) methodology which comprises three steps. (1) CA synthesizes distinct ID and OOD samples by adeptly transforming OOD samples to their ID analogs, applicable in scenarios with and without access to training ID data (Section 4.1). (2) The predicted label distributions from these synthesized samples undergo adjustments through a uniform distribution and a weight function, intentionally fostering low confidence for OOD and heightened confidence for ID samples (Section 4.2). (3) These samples, with their adjusted predicted label distributions, are harnessed to train an OOD-sensitive binary classifier, tasked with discerning between ID and OOD samples for the standard network (Section 4.3).

data is generated to match the feature statistics of the original dataset. Another influential work by Lopes et al. [Lopes, Fenu, and Starner \(2017\)](#) uses a series of transformations to generate data that resembles the original training set. Additionally, Haroush et al. [Heo, Lee, Yun, and Choi \(2019\)](#) recently showcased a method that iteratively refines synthetic samples, enhancing the quality of distillation. Traditional knowledge distillation and data-free distillation primarily concern transferring ID classification knowledge from one network, often a more complex one, to a lighter-weight network that also emphasizes classification tasks. In contrast, our proposed learning framework, termed OOD knowledge distillation, seeks to convey OOD-sensitive knowledge from one network to another, with the specific aim of differentiating between ID and OOD samples.

2.3 Data Synthesis

A variety of methods have been proposed to synthesize artificial data that closely mirrors real-world data. Variational Autoencoder (VAE) [Kingma and Welling \(2014\)](#) is a generative model that learns to encode input data into a latent space and then decodes to produce new data samples that mirror the input distribution. Generative Adversarial Networks (GAN) [Goodfellow et al. \(2014\)](#) employs a dual network structure, where a generator crafts synthetic data while a discriminator assesses its authenticity, collaboratively

refining the generation process. DeepDream [Mordvintsev et al. \(2015\)](#) iteratively modifies images to enhance the patterns recognized by a neural network, leading to dream-like generated images. DeepInversion [Yin et al. \(2020\)](#) inverts the roles in the training process, aiming to generate images that maximize the response of particular neurons, providing insights into what deep networks perceive. Existing data synthesis methods primarily focus on the final generated samples. However, our algorithm emphasizes the entire generation process where samples gradually transition from OOD to ID, with their confidence levels steadily increasing. Every sample produced throughout this process is fully utilized by our approach.

3 OOD Knowledge Distillation

A standard network, denoted as $\mathcal{P}_\theta(y|\mathbf{x})$ and parameterized by θ , is trained using an ID dataset $\mathbf{O} = \{(\mathbf{x}_i, y_i)\}_{i=1}^N$. This dataset consists of N independent and identically distributed samples drawn from an unknown distribution. In this notation, $\mathbf{x} \in \mathcal{X}$ represents the input, $y \in [K]$ is the associated label, with K being the total number of labels. OOD knowledge distillation extracts knowledge from the standard network $\mathcal{P}_\theta(y|\mathbf{x})$ to train its specialized binary classifier, tailored to discriminate between ID and OOD samples.

Specifically, for a given standard network $\mathcal{P}_\theta(y|\mathbf{x})$, the OOD knowledge distillation procedure begins by synthesizing a dataset $\mathbf{S} = \{\hat{\mathbf{x}}_i\}_{i=1}^M$ and extracting their corresponding predicted label distributions from the standard network. Following this, these distributions are adjusted by combining with OOD prior knowledge and adaptive weights for training the binary classifier $\mathcal{P}_\phi(c|\mathbf{x})$, parameterized by ϕ , where $c \in \{0, 1\}$. Here, $c = 1$ signifies that the test sample \mathbf{x} is ID, while $c = 0$ indicates an OOD sample. In the testing phase, the classifier $\mathcal{P}_\phi(c|\mathbf{x})$ determines whether a given input \mathbf{x} is ID or OOD. If identified as ID, the standard network $\mathcal{P}_\theta(y|\mathbf{x})$ is utilized to predict its label. Conversely, if it is determined to be OOD, the standard network abstains from making a label prediction.

4 Confidence Amendment

Confidence Amendment (CA), visualized in Fig. 2, is designed to address the challenges associated with OOD knowledge distillation, specifically those involving the extraction of knowledge from a standard network and the subsequent refinement of this knowledge for training an OOD-sensitive binary classifier. CA generates ID and OOD samples for the standard network by progressively converting OOD samples into ID samples through the enhancement of confidence levels. Following this process, CA retrieves the predicted label distributions for the synthesized samples from the standard network and linearly combines these distributions with a uniform distribution, utilizing adaptive weights. The synthesized samples, together with the adjusted predicted label distributions, are then used to train a binary classifier, which is tasked with distinguishing between ID and OOD samples.

4.1 Synthesizing Training Data

CA synthesizes samples, including both ID and OOD samples, through a parameterized Markov chain. In the transitions within this chain, an OOD sample is gradually converted into an ID sample by elevating its confidence with respect to the standard network $\mathcal{P}_\theta(y|\mathbf{x})$. Consequently, specific ID and OOD samples for the standard network can be effectively synthesized.

Accordingly, a random noise $\hat{\mathbf{x}}_0$ drawn from a standard distribution $\mathcal{N}(\mathbf{0}, \mathbf{I})$ can be considered an OOD sample, as the training ID samples from \mathbf{O} do not follow this standard distribution, i.e.,

$$\hat{\mathbf{x}}_0 \sim \mathcal{N}(\mathbf{0}, \eta \mathbf{I}). \quad (1)$$

Taking inspiration from diffusion probabilistic models Ho et al. (2020); Sohl-Dickstein et al. (2015), the randomly-initialized OOD sample incrementally transitions to an ID sample after T transformations within a Markov chain, defined as follows:

$$\mathcal{P}_t(\hat{\mathbf{x}}_t|\hat{\mathbf{x}}_{t-1}) = \mathcal{N}(\boldsymbol{\mu}_t, \eta \mathbf{I}), \quad t \in [1, T], \quad (2)$$

where η is the variance, $\boldsymbol{\mu}_t$ is the expectation of $\hat{\mathbf{x}}_t$, and T represents the maximum transition time. To facilitate the evolution of an OOD sample into an ID sample for the standard network, the confidence level of the sample needs enhancement, as ID samples typically exhibit high-confidence predictions. Drawing from the principles of adversarial sample generation models Goodfellow et al. (2015), the confidence of a randomly-initialized OOD sample can be boosted by introducing a small, informative perturbation that relates to both the standard network and a random label. Consequently, the expectation $\boldsymbol{\mu}_t$ can be expressed as:

$$\boldsymbol{\mu}_t = \hat{\mathbf{x}}_{t-1} - \rho \nabla G_\theta(\hat{\mathbf{x}}_{t-1}). \quad (3)$$

Here, ρ is a coefficient denoting the magnitude of the perturbation. The term $G_\theta(\hat{\mathbf{x}})$ is based on the standard network $\mathcal{P}_\theta(y|\hat{\mathbf{x}})$ and incorporates a regularizer $\mathcal{R}(\hat{\mathbf{x}})$ applied to the synthesized sample $\hat{\mathbf{x}}$, formulated as:

$$G_\theta(\hat{\mathbf{x}}) = -\log \mathcal{P}_\theta(y|\hat{\mathbf{x}}) + \mathcal{R}(\hat{\mathbf{x}}), \quad (4)$$

where $\mathcal{R}(\hat{\mathbf{x}})$ encourages the distribution of synthesized samples to closely align with that of the original training samples.

Specifically, when the training dataset \mathbf{O} is available, inspired by the concept of the variational autoencoder Kingma and Welling (2014), the distribution discrepancy between the real and synthesized samples can be minimized. Accordingly, the regularizer $\mathcal{R}(\hat{\mathbf{x}})$ applicable when the training datasets are available, which is termed

DeepRecon, can be defined as follows:

$$\mathcal{R}(\widehat{\mathbf{x}}) = \mathcal{R}^+(\widehat{\mathbf{x}}) = \beta_{\text{MSE}} \text{MSE}(\widehat{\mathbf{x}}, \mathbf{x}), \quad (5)$$

where MSE represents the mean squared error scaled by factor β_{MSE} , and \mathbf{x} is a sample randomly selected from the training dataset \mathbf{O} . Additionally, the label used in the standard network $\mathcal{P}_\theta(y|\widehat{\mathbf{x}})$ in the computation of $G_\theta(\widehat{\mathbf{x}})$ is the ground-truth label y corresponding to the randomly-selected \mathbf{x} . Alternatively, when the training dataset \mathbf{O} is unavailable, one can regularize the distribution of synthesized samples by using priors, a strategy inspired by DeepDream [Mordvintsev et al. \(2015\)](#) and DeepInversion [Yin et al. \(2020\)](#), which ensures stable convergence towards valid samples. In this case, the regularizer $\mathcal{R}(\widehat{\mathbf{x}})$ for unavailable training datasets can be expressed as:

$$\mathcal{R}(\widehat{\mathbf{x}}) = \mathcal{R}^-(\widehat{\mathbf{x}}) = \beta_{\text{TV}} \mathcal{R}_{\text{TV}}(\widehat{\mathbf{x}}) + \beta_{l_2} \mathcal{R}_{l_2}(\widehat{\mathbf{x}}) + \beta_f \mathcal{R}_f(\widehat{\mathbf{x}}), \quad (6)$$

where $\mathcal{R}_{\text{TV}}(\widehat{\mathbf{x}})$, $\mathcal{R}_{l_2}(\widehat{\mathbf{x}})$, and $\mathcal{R}_f(\widehat{\mathbf{x}})$ penalize the total variance, l_2 norm, and the distribution of intermediate feature maps of $\widehat{\mathbf{x}}$, respectively, each scaled by their corresponding factors β_{TV} , β_{l_2} , and β_f . The three regularization terms are introduced in DeepInversion [Yin et al. \(2020\)](#).

As per Eq. (2), Eq. (3), and Eq. (4), coupled with the application of the reparameterization trick [Gal and Ghahramani \(2016\)](#), the synthesized sample $\widehat{\mathbf{x}}_t$ at time $t \in [1, T]$ within the parameterized Markov chain can be determined in closed form as follows:

$$\widehat{\mathbf{x}}_t = \widehat{\mathbf{x}}_{t-1} + \rho \nabla \log \mathcal{P}_\theta(y|\widehat{\mathbf{x}}_{t-1}) - \rho \nabla \mathcal{R}(\widehat{\mathbf{x}}_{t-1}) + \eta \mathbf{z}, \quad (7)$$

where \mathbf{z} is a random variable following a standard distribution, i.e., $\mathbf{z} \sim \mathcal{N}(\mathbf{0}, \mathbf{I})$. Given a random initial dataset $\mathbf{S}_0 = \{\widehat{\mathbf{x}}_{i,0}\}_{i=1}^N$ consisting of N independent random variables drawn from $\mathcal{N}(\mathbf{0}, \mathbf{I})$, the corresponding synthesized data subset $\mathbf{S}_t = \{\widehat{\mathbf{x}}_{i,t}\}_{i=1}^N$ at time $t \in [1, T]$ can be derived through Eq. (7). Consequently, by aggregating all such datasets across the various time steps, we obtain the synthesized dataset:

$$\mathbf{S} = \bigcup_{t=0}^T \mathbf{S}_t = \{\widehat{\mathbf{x}}_{i,0:T}\}_{i=1}^N, \quad (8)$$

which encompasses $N(T+1)$ samples. Notably, the OOD samples present at time 0 gradually evolve

into ID samples as time progresses to T . Therefore, the dataset \mathbf{S} encapsulates both distinct OOD and ID samples pertinent to the standard network $\mathcal{P}_\theta(y|\mathbf{x})$.

4.2 Adjusting Predicted Label Distributions

For samples originating from the synthesized dataset \mathbf{S} , their predicted label distributions can be retrieved from the standard network $\mathcal{P}_\theta(y|\mathbf{x})$. Samples in \mathbf{S} with few transitions can be regarded as OOD, owing to the substantial discrepancy between their distribution and that of the ID. However, as illustrated in Fig. 1, these samples might receive unexpectedly high-confidence predictions from the standard network, despite their characteristics. This phenomenon arises due to the distributional vulnerability of the standard network [Zhao et al. \(2023b\)](#). While the network is trained on ID samples, it does not have constraints imposed on OOD samples. This can lead to uncertain and occasionally high-confidence predictions for OOD samples. Thus, utilizing the synthesized samples and their predicted label distributions from the standard network directly for training a binary classifier would not enhance the OOD sensitivity of the network.

To improve OOD sensitivity, refining the extracted knowledge by adjusting the predicted label distributions of synthesized samples is necessary, ensuring that OOD samples correlate with low-confidence predictions. The fundamental idea behind this approach is to incrementally place trust in the prediction confidence. Specifically, in the process of synthesizing samples, earlier samples are more likely to be OOD, and therefore their high-confidence predictions are not reliable. In contrast, later samples tend to be ID, and their high-confidence predictions are reliable. Therefore, for a synthesized sample $\widehat{\mathbf{x}}_{i,t}$ at time t , with $i \in [N]$ and $t \in [0, T]$, the adjusted predicted label distribution can be computed as:

$$\mathcal{Q}_\theta(y|\widehat{\mathbf{x}}_{i,t}) = \alpha(t)\mathcal{U} + (1 - \alpha(t))\mathcal{P}_\theta(y|\widehat{\mathbf{x}}_{i,t}), \quad (9)$$

where \mathcal{U} denotes the uniform distribution and α represents a weight function defined as:

$$\alpha(t) = \left(\frac{t}{T}\right)^a, \quad a \geq 0. \quad (10)$$

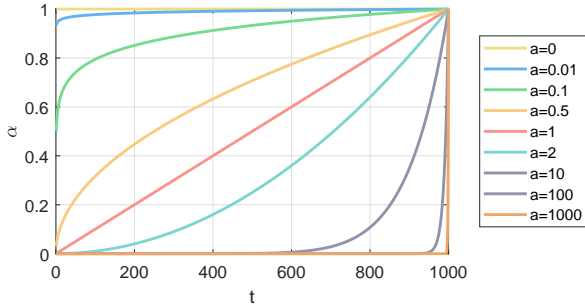


Fig. 3 Curves of the function $\alpha(t)$ under different parameters. Best viewed in color.

Fig. 3 displays the curves of the weight function for various coefficients of $a \geq 0$. When $a = 0$, all function values are unity, suggesting complete reliance of the synthesized samples on the confidence provided by the standard network. For $a > 0$, the function exhibits a monotonic increase, indicating that the synthesized samples will progressively trust the confidence levels from the standard network, with higher trust accorded as a sample approaches ID characteristics. Consequently, with $a > 0$, confidence levels from the standard network are revised in the process of confidence amendment, assigning lower confidence to OOD samples and higher confidence to ID samples, thereby heightening OOD sensitivity.

4.3 Training OOD-sensitive Binary Classifier

To harness the deeper knowledge encapsulated within the standard network $\mathcal{P}_\theta(y|\mathbf{x})$, for a given input \mathbf{x} , we aim to map it to the adjusted predicted label distribution $\mathcal{Q}_\theta(y|\mathbf{x})$ using an auxiliary network $\mathcal{P}_\phi(y|\mathbf{x})$ parameterized by ϕ . Subsequently, a specialized binary classifier capable of distinguishing between ID and OOD samples can be devised based on this auxiliary network. Following conventional knowledge distillation approaches, OOD-sensitive information from $\mathcal{Q}_\theta(y|\mathbf{x})$ can be transferred to $\mathcal{P}_\phi(y|\mathbf{x})$ by optimizing the objective

$$\min_{\phi} \sum_{\mathbf{x} \in \mathbf{S}} \sum_{y \in [K]} \mathcal{D}_{\text{KL}}(\mathcal{P}_\phi(y|\mathbf{x}) || \mathcal{Q}_\theta(y|\mathbf{x})), \quad (11)$$

where $\mathcal{D}_{\text{KL}}(\cdot || \cdot)$ denotes the Kullback-Leibler divergence. Inspired by the maximum over softmax probability technique [Hendrycks and Gimpel](#)

(2017), which computes an OOD score for a test sample based on prediction confidence, we can formulate the specialized binary classifier for the standard network $\mathcal{P}_\theta(y|\mathbf{x})$ using the auxiliary network $\mathcal{P}_\phi(y|\mathbf{x})$:

$$\begin{aligned} \mathcal{P}_\phi(c = 1|\mathbf{x}) &= \max_{y \in [K]} \mathcal{P}_\phi(y|\mathbf{x}), \\ \mathcal{P}_\phi(c = 0|\mathbf{x}) &= 1 - \max_{y \in [K]} \mathcal{P}_\phi(y|\mathbf{x}), \end{aligned} \quad (12)$$

with $c = 1$ signifying that the test sample \mathbf{x} is ID and $c = 0$ denoting an OOD sample. Thus, $\mathcal{P}_\phi(c|\mathbf{x})$ acts as the specialized binary classifier corresponding to the standard network $\mathcal{P}_\theta(y|\mathbf{x})$. This classifier, trained with specific samples derived from the standard network, is tailored to differentiate between ID and OOD, exhibiting sensitivity to the latter. During testing, for a given sample \mathbf{x} , the value of $\mathcal{P}_\phi(c = 0|\mathbf{x})$ serves as the OOD score. A higher score suggests a greater likelihood that the sample is OOD. The process of training this specialized binary classifier, known as Confidence Amendment (CA), is outlined in Algorithm 1.

5 Theoretical Guarantees

To elucidate how the weight function α enhances OOD sensitivity, we derive the generalization error bound of the specialized binary classifier $\mathcal{P}_\phi(c|\mathbf{x})$ in distinguishing between ID and OOD samples. For convenience, we assume the hypothesis space of the specialized binary classifiers $\mathcal{P}_\phi(c|\mathbf{x})$ is denoted as \mathcal{H} , then we have

$$h(\mathbf{x}) = \mathcal{P}_\phi(c = 0|\mathbf{x}). \quad (13)$$

Let $\mathcal{P}_{\mathbf{S}}$ represent the mixture distribution of ID and OOD samples drawn from \mathbf{S} , and define $l(h(\mathbf{x}), c) = \mathbf{I}[h(\mathbf{x}) = c]$ as the 0-1 loss function. Then, the expected risk of $h(\mathbf{x})$ can be expressed as:

$$\mathcal{L}_{\mathcal{P}}[h] = \int_{\mathcal{P}} l(h(\mathbf{x}), c) d\mathbf{x}, \quad (14)$$

with its empirical risk given by

$$\mathcal{L}_{\mathbf{S}}[h] = \frac{1}{|\mathbf{S}|} \sum_{\mathbf{x} \sim \mathbf{S}} l(h(\mathbf{x}), c). \quad (15)$$

We proceed to analyze the generalization error bound of the specialized binary classifier, drawing

Algorithm 1 Confidence Amendment (CA)

Require: Standard network $\mathcal{P}_\theta(y|\mathbf{x})$, weight function coefficient a , maximum transition time T

1: Synthesize a dataset \mathbf{S} by integrating samples at $t \in [0, T]$ in the Markov chain:

$$\widehat{\mathbf{x}}_t = \widehat{\mathbf{x}}_{t-1} + \rho \nabla \log \mathcal{P}_\theta(y|\widehat{\mathbf{x}}_{t-1}) - \rho \nabla \mathcal{R}(\widehat{\mathbf{x}}_{t-1}) + \eta \mathbf{z}.$$

2: For each synthesized sample $\widehat{\mathbf{x}}_{i,t} (i \in [N], t \in [0, T])$ in \mathbf{S} , adjust the predicted label distribution:

$$\mathcal{Q}_\theta(y|\widehat{\mathbf{x}}_{i,t}) = \alpha(t)\mathcal{U} + (1 - \alpha(t)) \mathcal{P}_\theta(y|\widehat{\mathbf{x}}_{i,t}).$$

3: Distill knowledge from $\mathcal{Q}_\theta(y|\mathbf{x})$ into auxiliary network $\mathcal{P}_\phi(y|\mathbf{x})$ by optimizing:

$$\min_{\phi} \sum_{\mathbf{x} \in \mathbf{S}} \sum_{y \in [K]} \mathcal{D}_{\text{KL}}(\mathcal{P}_\phi(y|\mathbf{x}) || \mathcal{Q}_\theta(y|\mathbf{x})).$$

4: Formulate specialized binary classifier $\mathcal{P}_\phi(c|\mathbf{x})$ based on auxiliary network $\mathcal{P}_\phi(y|\mathbf{x})$:

$$\mathcal{P}_\phi(c = 1|\mathbf{x}) = \max_{y \in [K]} \mathcal{P}_\phi(y|\mathbf{x}), \mathcal{P}_\phi(c = 0|\mathbf{x}) = 1 - \max_{y \in [K]} \mathcal{P}_\phi(y|\mathbf{x}).$$

Ensure: OOD-sensitive binary classifier $\mathcal{P}_\phi(c|\mathbf{x})$

on shattering dimensions and covering numbers. This analysis will commence with the definitions and corresponding lemmas related to these concepts. The methods of proving the generalization error bound in this paper are based on Vapnik's method of structural risk minimisation [Shawe-Taylor, Bartlett, Williamson, and Anthony \(1998\)](#). **Definition 1** (Fat Shattering Dimension [Kearns and Schapire \(1994\)](#)). Let \mathcal{H} be a set of real-valued functions. A set of points \mathcal{X} is said to be γ -shattered by \mathcal{H} if there exist real numbers $r_{\mathbf{x}}$, each indexed by $\mathbf{x} \in \mathcal{X}$, such that for all binary vectors b , also indexed by \mathbf{x} , there exists a function $h_b \in \mathcal{H}$ satisfying

$$h_b(\mathbf{x}) = \begin{cases} r_{\mathbf{x}} + \gamma & \text{if } b_{\mathbf{x}} = 1, \\ r_{\mathbf{x}} - \gamma & \text{otherwise.} \end{cases}$$

The fat-shattering dimension denoted as $\text{fat}_{\mathcal{H}}$, of the set \mathcal{H} is a function mapping positive real numbers to integers. Specifically, it assigns a value γ to the size of the largest set \mathcal{X} that is γ -shattered by \mathcal{H} , yielding infinity if no such finite set exists.

Definition 2 (ϵ -covering [Shalev-Shwartz and Ben-David \(2014\)](#)). Let (\mathcal{X}, d) be a (pseudo-)metric space and \mathcal{A} a subset of \mathcal{X} with a specified $\epsilon > 0$. A set $\mathcal{B} \subseteq \mathcal{A}$ is called an ϵ -cover for \mathcal{A} if, for every element $A \in \mathcal{A}$, there exists an element $B \in \mathcal{B}$

satisfying $d(A, B) \leq \epsilon$. The ϵ -covering number of \mathcal{A} , denoted as $N(\epsilon, \mathcal{A})$, represents the minimal cardinality of an ϵ -cover for \mathcal{A} . This number is defined to be infinite (∞) if no finite ϵ -cover exists for \mathcal{A} .

Lemma 1 (Covering Number [Shawe-Taylor et al. \(1998\)](#)). Let \mathcal{H} be a class of functions mapping $\mathcal{X} \rightarrow [b_1, b_2]$, and let $\mathcal{P}_{\mathcal{X}}$ represent a distribution over \mathcal{X} . Given $0 < \epsilon < 1$, set $\kappa = \text{fat}_{\mathcal{H}}(\epsilon/4)$. Then, the expectation

$$\mathbb{E}_{\mathcal{X}^m} (\mathfrak{N}(\epsilon, \mathcal{H})) \leq 2 \left(\frac{4m(b_2 - b_1)^2}{\epsilon^2} \right)^{\kappa \log \frac{2em(b_2 - b_1)}{\kappa \epsilon}}$$

is taken over m samples $\mathbf{S} \in \mathcal{X}^m$ drawn in accordance with the distribution $\mathcal{P}_{\mathcal{X}}$.

Lemma 2 (Symmetrization [V. Vapnik \(2006\)](#)). Let \mathcal{H} be a class of real-valued functions and let $\mathcal{P}_{\mathcal{X}}$ be a probability measure on \mathcal{X} . Let \mathbf{S} and $\bar{\mathbf{S}}$ each contain m samples, both drawn independently according to $\mathcal{P}_{\mathcal{X}}$. If $m > 2/\epsilon$, then we have

$$\begin{aligned} & \mathcal{P}_{\mathbf{S}} \left(\sup_{h \in \mathcal{H}} |\mathcal{L}_{\mathbf{S}}[h] - \mathcal{L}_{\mathcal{P}}[h]| \geq \epsilon \right) \\ & \leq \mathcal{P}_{\mathbf{S}\bar{\mathbf{S}}} \left(\sup_{h \in \mathcal{H}} |\mathcal{L}_{\mathbf{S}}[h] - \mathcal{L}_{\bar{\mathbf{S}}}[h]| \geq \epsilon/2 \right). \end{aligned}$$

Lemma 3 (Fat Shattering Dimension Bound [Bartlett and Shawe-Taylor \(1999\)](#)). *Suppose \mathcal{H} is confined to points within an n -dimensional ball of radius R centered at the origin. Then, we have*

$$\text{fat}_{\mathcal{H}}(\gamma) \leq \min \left\{ \frac{R^2}{\gamma^2}, n + 1 \right\}.$$

Building upon the aforementioned definitions and lemmas, we propose the subsequent theorem, which provides an empirical risk bound for a hypothesis $h \in \mathcal{H}$. This bound is applicable to a dataset comprising both ID and OOD samples, under the condition that h can perfectly classify samples within the training dataset.

Theorem 1. *Consider a hypothesis $h \in \mathcal{H}$ that maps \mathcal{X} to \mathbb{R} and possesses margins $\{\gamma_t\}_{t=0}^T$ on the dataset $\mathbf{S} = \{\mathbf{S}_t\}_{t=0}^T$. Suppose the finite fat-shattering dimension of each margin is bounded by the function $\kappa_t = \text{fat}(\gamma_t/8)$, which is continuous from the right. Given two distinct datasets \mathbf{S} and $\bar{\mathbf{S}}$ consisting of $M = N(T+1)$ synthesized samples and for any $\delta > 0$, we obtain*

$$\mathcal{P}^{2M} \{ \mathbf{S}\bar{\mathbf{S}} : \exists h \in \mathcal{H}, \mathcal{L}_{\mathbf{S}}[h] = 0, \kappa_{0:T}, \mathcal{L}_{\bar{\mathbf{S}}}[h] > \varepsilon_{\bar{\mathbf{S}}} \} < \delta,$$

where

$$\varepsilon_{\bar{\mathbf{S}}} = \frac{\log(32M) \sum_{t=0}^T \kappa_t \log(8eM)}{M} + \frac{1}{M} \log \frac{2}{\delta}.$$

Proof. According to the standard permutation argument [V.N. Vapnik and Chervonenkis \(2015\)](#), the probability can be bounded by the fixed sequence $\mathbf{S}\bar{\mathbf{S}}$ and its corresponding permuted sequence. For datasets $\mathbf{S}_t = \{\mathbf{x}_{i,t}\}_{i=1}^N \subseteq \mathbf{S}$ and $\bar{\mathbf{S}}_t = \{\bar{\mathbf{x}}_{i,t}\}_{i=1}^N \subseteq \bar{\mathbf{S}}$ where $t \in [0, T]$, we define their corresponding datasets with the second component determined by the target value of the first component, i.e.,

$$\mathbf{Z}_t = \{(\mathbf{x}_{i,t}, c_{i,t})\}_{i=1}^N, \mathbf{Z} = \bigcup_{t=0}^T \mathbf{Z}_t,$$

$$\bar{\mathbf{Z}}_t = \{(\bar{\mathbf{x}}_{i,t}, \bar{c}_{i,t})\}_{i=1}^N, \bar{\mathbf{Z}} = \bigcup_{t=0}^T \bar{\mathbf{Z}}_t.$$

Accordingly, for a hypothesis $h \in \mathcal{H}$, we transform the problem of observing the maximal value taken by a set of functions by considering its corresponding function $\hat{h} \in \hat{\mathcal{H}}$ for any $\zeta \geq 1$,

$$h(\mathbf{x}) \mapsto \hat{h}(\mathbf{x}, c) = (2\zeta - h(\mathbf{x}))(1 - c) + h(\mathbf{x})c.$$

For \mathbf{z}_t , we define that

$$r_t = \max_{(\mathbf{x}, c) \in \mathbf{z}_t} \hat{h}(\mathbf{x}_{i,t}, c_i).$$

Accordingly, at least $N\varepsilon_{\bar{\mathbf{S}}}$ samples $(\bar{\mathbf{x}}, \bar{c}) \in \bar{\mathbf{Z}}_t$ satisfy

$$\hat{h}(\bar{\mathbf{x}}, \bar{c}) \geq r_t + 2\hat{\gamma}_t.$$

Let $\gamma_t = \min\{\gamma'_t : \text{fat}(\gamma'_t/4) \leq \kappa_t\}$, we have $\gamma_t \leq \hat{\gamma}_t$. Without loss of generality, we assume $\gamma_t = 2\hat{\gamma}_t$ and $\zeta = r_t + 2\hat{\gamma}_t$ according to [Definition 1](#).

For $t \in [0, T]$, we define the following probability event

$$\mathbf{Z}_t = \{ \mathbf{S}\bar{\mathbf{S}} : \exists h \in \mathcal{H}, \mathcal{L}_{\mathbf{S}}[h] = 0, \mathcal{C}_t^1, \mathcal{C}_t^2, \mathcal{C}_t^3 \},$$

$$\mathcal{C}_t^1 : r_t = \max_{(\mathbf{x}, c) \in \mathbf{Z}_t} \hat{h}(\mathbf{x}, c),$$

$$\mathcal{C}_t^2 : \zeta = r_t + 2\hat{\gamma}_t,$$

$$\mathcal{C}_t^3 : |\{(\bar{\mathbf{x}}, \bar{c}) \in \bar{\mathbf{Z}}_t : \hat{h}(\bar{\mathbf{x}}, \bar{c}) \geq 2\hat{\gamma}_t + r_t\}| > M\varepsilon_{\bar{\mathbf{S}}}.$$

and the following auxiliary function

$$\pi_t(\hat{h}) = \begin{cases} \zeta & \text{if } \hat{h} \geq \zeta \\ \zeta - 2\hat{\gamma}_t & \text{if } \hat{h} \leq \zeta - 2\hat{\gamma}_t, \\ \hat{h} & \text{otherwise} \end{cases}$$

and let $\pi_t(\hat{\mathcal{H}}) = \{\pi_t(\hat{h}) : \hat{h} \in \hat{\mathcal{H}}\}$. Consider the [Definition 2](#) and a minimal $\hat{\gamma}_t$ -cover \mathcal{B}_t of $\pi_t(\hat{\mathcal{H}})$, we have that for any $\hat{h} \in \hat{\mathcal{H}}$, there exists $\hat{h}_{\mathcal{B}_t} \in \hat{\mathcal{H}}_{\mathcal{B}_t}$, with

$$|\pi_t(\hat{h}(\mathbf{x}, c)) - \pi_t(\hat{h}_{\mathcal{B}_t}(\mathbf{x}, c))| < \hat{\gamma}_t, \forall (\mathbf{x}, c) \in \mathbf{Z}_t \cup \bar{\mathbf{Z}}_t.$$

Therefore, according to the definition of r_t , for all $(\mathbf{x}, c) \in \mathbf{Z}_t$, we have

$$\hat{h}(\mathbf{x}, c) \leq r_t = \zeta - 2\hat{\gamma}_t,$$

$$\pi_t(\hat{h}(\mathbf{x}, c)) = \zeta - 2\hat{\gamma}_t,$$

$$\pi_t(\hat{h}_{\mathcal{B}_t}(\mathbf{x}, c)) \leq \zeta - \hat{\gamma}_t.$$

Therefore, there are at least $M\varepsilon_{\mathcal{S}}$ samples $(\bar{\mathbf{x}}, \bar{c}) \in \bar{\mathcal{Z}}$ such that

$$\begin{aligned}\widehat{h}(\bar{\mathbf{x}}, \bar{c}) &\geq \zeta = r_t + 2\widehat{\gamma}_t, \\ \pi_t(\widehat{h}_{\mathcal{B}_t}(\bar{\mathbf{x}}, \bar{c})) &\geq \zeta - \widehat{\gamma}_t \geq \max_{(\mathbf{x}, c) \in \mathcal{Z}_t} \pi_t(\widehat{h}_{\mathcal{B}_t}(\mathbf{x}, c)).\end{aligned}$$

Since π_t only reduces the separation between output values, we have

$$\pi_t(\widehat{h}_{\mathcal{B}_t}(\bar{\mathbf{x}}, \bar{c})) > \pi_t(\widehat{h}_{\mathcal{B}_t}(\mathbf{x}, c)), \forall (\mathbf{x}, c) \in \mathcal{Z}_t, \forall (\bar{\mathbf{x}}, \bar{c}) \in \bar{\mathcal{Z}}.$$

According to the permutation argument, there are at most $2^{-M\varepsilon_{\mathcal{S}}}$ of sequences obtained by swapping corresponding points satisfying conditions for a fixed $\widehat{h}_{\mathcal{B}_t} \in \widehat{\mathcal{H}}_{\mathcal{B}_t}$. This is because the $M\varepsilon_{\mathcal{S}}$ points with the largest $\widehat{h}_{\mathcal{B}_t}$ values must remain for the inequality occur. Therefore, for any $h \in \mathcal{H}$, there are at least \mathcal{B}_t hypothesis $\widehat{h}_{\mathcal{B}_t} \in \widehat{\mathcal{H}}_{\mathcal{B}_t}$ satisfying the inequality for $\widehat{\gamma}_t$.

Every set of points $\widehat{\gamma}_t$ -shattered by $\pi_t(\widehat{\mathcal{H}})$ can be $\widehat{\gamma}_t$ -shattered by $\widehat{\mathcal{H}}$, which indicates that $\text{fat}_{\pi_t(\widehat{\mathcal{H}})}(\widehat{\gamma}_t) \leq \text{fat}_{\widehat{\mathcal{H}}}(\widehat{\gamma}_t)$. Applying Lemma 1 for $\pi_t(\widehat{\mathcal{H}}) \in [\zeta - 2\widehat{\gamma}_t, \zeta]$, we obtain

$$\begin{aligned}\mathbb{E}_{\mathcal{Z}\bar{\mathcal{Z}}}(|\mathcal{B}_t|) &= \mathbb{E}_{\mathcal{Z}\bar{\mathcal{Z}}}(\mathfrak{N}(\widehat{\gamma}_t, \pi_t(\widehat{\mathcal{H}}))) \\ &\leq 2(32M)^{\kappa_t \log \frac{8eM}{\kappa_t}} \leq 2(32M)^{\kappa_t \log(8eM)}.\end{aligned}$$

According to the union bound, we have

$$\begin{aligned}&\mathcal{P}^{2M} \{ \mathcal{S}\bar{\mathcal{S}} : \exists h \in \mathcal{H}, \mathcal{L}_{\mathcal{S}}[h] = 0, \kappa_{0:T}, \mathcal{L}_{\mathcal{S}}[h] > \varepsilon_{\mathcal{S}} \} \\ &\leq \mathcal{P} \left(\bigcup_{t=0}^T \mathcal{Z}_t \right) \leq \sum_{t=0}^T \mathcal{P}(\mathcal{Z}_t) \leq \sum_{t=0}^T \mathbb{E}_{\mathcal{Z}\bar{\mathcal{Z}}}(|\mathcal{B}_t|) 2^{-M\varepsilon_{\mathcal{S}}} \\ &\leq 2^{-M\varepsilon_{\mathcal{S}}} \sum_{t=0}^T 2(32M)^{\kappa_t \log(8eM)} \leq \delta.\end{aligned}$$

According to the convex function properties and Jensen inequality, we have

$$2^{-M\varepsilon_{\mathcal{S}}} 2 \sum_{t=0}^T \kappa_t \log(8eM) \leq \delta$$

Accordingly, the inequality holds if

$$\varepsilon_{\mathcal{S}} = \frac{\log(32M) \sum_{t=0}^T \kappa_t \log(8eM)}{M} + \frac{1}{M} \log \frac{2}{\delta}.$$

□

Drawing upon the empirical risk bound delineated in Theorem 1, we are positioned to derive the expected risk bound. This derivation is pertinent when there is a binary classifier at play, capable of classifying samples from the training dataset flawlessly. That is, achieving a zero empirical risk. The focus here is on establishing a bound on the generalization error, which is accomplished by uniformly bounding the probabilities across all conceivable margins.

Theorem 2. Consider a hypothesis space \mathcal{H} restricted to a ball of radius R . Let $h \in \mathcal{H}$ be a hypothesis that accurately classifies $M = N(T+1)$ samples from $\mathcal{S} \in \mathcal{P}$, with a margin of $\gamma_t = \zeta - r_t$ and fat dimension $\kappa_t = \text{fat}(\gamma_t/8)$ for each dataset \mathcal{S}_t assigned to K classes. Here, $\zeta \geq 1$, $r_t = \max_{\mathbf{x} \in \mathcal{S}_t} h(\mathbf{x})$, and $t \in [0, T]$. With a probability of at least $1 - \delta$, the generalization error bound is given by:

$$\mathcal{L}_{\mathcal{P}}[h] \leq \frac{620R^2 \log(32M)}{\sqrt{M^3} \sum_{t=0}^T (\zeta - r_t)^2} + \frac{9}{\sqrt{N}\delta}.$$

Proof. The uniform convergence bound of the generalization error is defined as

$$\begin{aligned}&\mathcal{P}_{\mathcal{S}} \left(\sup_{h \in \mathcal{H}} \mathcal{L}_{\mathcal{S}}[h] - \mathcal{L}_{\mathcal{P}}[h] \geq \varepsilon_{\mathcal{P}} \right) \\ &\leq \mathcal{P}_{\mathcal{S}\bar{\mathcal{S}}} \left(\sup_{h \in \mathcal{H}} |\mathcal{L}_{\mathcal{S}}[h] - \mathcal{L}_{\bar{\mathcal{S}}}[h]| \geq \varepsilon_{\mathcal{P}}/2 \right) \\ &\leq \mathcal{P}^{2M} \left(\bigcup_{\kappa_0=1}^{2N} \dots \bigcup_{\kappa_T=1}^{2N} J(\kappa_{0:T}) \right) \\ &\leq \sum_{\kappa_0=1}^{2N} \dots \sum_{\kappa_T=1}^{2N} \mathcal{P}^{2M} J(\kappa_{0:T}),\end{aligned} \tag{16}$$

where $J(\kappa_{0:T})$ is defined as

$$\mathcal{P}^{2M} \{ \mathcal{S}\bar{\mathcal{S}} : \exists h \in \mathcal{H}, \mathcal{L}_{\mathcal{S}}[h] = 0, \kappa_{0:T}, \mathcal{L}_{\bar{\mathcal{S}}}[h] > \varepsilon_{\mathcal{S}} \}.$$

The first inequality arises from Lemma 2. The second inequality holds since the maximum value of $\kappa_t (t \in [0, T])$ is $2N$; specifically, it is impossible to shatter a greater number of points from $\mathcal{S}_t \cup \bar{\mathcal{S}}_t$. The third inequality is derived from the union bound. Let $\delta' = \delta/(2N)^{T+1}$. Then, we have

$$\mathcal{P}^{2M} (J(\kappa_{0:T})) \leq \delta'/(2N)^{T+1} = \delta. \tag{17}$$

Applying Lemma 3, we obtain

$$\kappa_t < \frac{(8 + \omega)R^2}{(\zeta - r_t)^2} < \frac{66R^2}{(\zeta - r_t)^2}, \quad (18)$$

where $\omega > 0$ is a small constant ensuring continuity from the right, a condition of this lemma. Without loss of generality, we set $\omega = 0.1$. Combining Eq. (16), Eq. (17), Eq. (18), and Theorem 1, with probability at least $1 - \delta$, we have

$$\mathcal{L}_{\mathcal{P}}[h] \leq \frac{132R^2 \log(8eM) \log(32M)}{M \sum_{t=0}^T (\zeta - r_t)^2} + \frac{6}{N} \log \frac{2N}{\delta}.$$

We complete the proof by applying the Jensen inequality and the following fundamental logarithm inequality to simplify this bound:

$$\log(x) \leq \frac{x-1}{\sqrt{x}} \leq \frac{x}{\sqrt{x}}, \forall x \geq 1.$$

□

Theorem 2 indicates that the generalization error bound is correlated with the margins over data subsets at different times t , with these margins being determined by the weight function. Consequently, we introduce the weight function $\alpha(t) = \left(\frac{t}{T}\right)^a$ for $t \in [0, T]$ to derive a more specific generalization error bound.

Corollary 1. *Under the stipulations of Theorem 2, consider $\alpha(t) = \left(\frac{t}{T}\right)^a$ for $t \in [0, T]$ as a weight function employed to smooth the output distribution of a standard network, with $a \geq 0$. With probability at least $1 - \delta$, the approximate generalization error bound is given by*

$$\mathcal{L}_{\mathcal{P}}[h] \leq \frac{620R^2 \log(32M) K^2 \varphi(a)}{4T\sqrt{M^3}(K-1)^2} + \frac{9}{\sqrt{N}\delta},$$

where

$$\varphi(a) = \frac{(a+1)(2a+1)}{a^2}.$$

Proof. Let's apply $\alpha_t = \left(\frac{t}{T}\right)^a$ as the weight function. For a given hypothesis $h \in \mathcal{H}$ and an input $\mathbf{x}_t \in \mathbf{S}_t$, the target value is given by

$$\begin{aligned} r_t &= \max_{\mathcal{P}_{\theta}(y|\mathbf{x}_t)} \mathbb{E}_{\mathbf{u} \sim \mathcal{U}} \left[\max_{y \in [K]} \alpha_t \mathbf{u} + (1 - \alpha_t) \mathcal{P}_{\theta}(y|\mathbf{x}_t) \right] \\ &= 1 - \left(1 - \frac{1}{K}\right) \alpha_t. \end{aligned}$$

Assuming $\zeta = 1 + \left(1 - \frac{1}{K}\right)$, we can express the sum as

$$\sum_{t=0}^T (\zeta - r_t)^2 = \left(1 - \frac{1}{K}\right)^2 \sum_{t=0}^T \underbrace{\left(1 - \left(\frac{t}{T}\right)^a\right)^2}_{v(t)}.$$

Since $v(t)$ is a monotonically decreasing and non-negative function, we can estimate the sum as follows:

$$\begin{aligned} \sum_{t=0}^T v(t) &\geq \int_0^{T+1} v(t) dt \geq \int_0^T v(t) dt \\ &= \frac{2Ta^2}{(a+1)(2a+1)}. \end{aligned}$$

□

Corollary 1 demonstrates that the weighting coefficient $a \geq 0$ in the weight function $\alpha(t)$ influences the generalization error bound of the specialized binary classifier through the function $\varphi(a)$. Given that

$$\frac{d\varphi(a)}{da} = \frac{-3a-2}{a^3} < 0, \forall a > 0, \quad (19)$$

$\varphi(a)$ is monotonically decreasing with respect to a . Therefore, by utilizing $M = N(T+1)$ synthesized samples from the parameterized Markov chain Eq. (7) and applying $\alpha_t = \left(\frac{t}{T}\right)^a$ to integrate knowledge from the standard network smoothly, the binary classifier that distinguishes between ID and OOD samples can achieve a lower generalization error bound when a larger weighting coefficient $a \geq 0$ is used.

6 Experiments

In this section, we evaluate the effectiveness of our proposed CA¹ approach by comparing its performance with state-of-the-art OOD detection methods, both with and without access to training ID data. We also conduct a parameter analysis, emphasizing the coefficient in the weight function to ensure its alignment with our theoretical guarantees and investigate the maximum transition time during the sample synthesis phase.

¹The source codes are available at: <https://github.com/Lawliet-zzl/CA>.

Furthermore, we delve into the effects of different regularization techniques on sample synthesis. Finally, we examine the transferability of the synthesized samples. In particular, we explore whether samples generated by a standard network can train a binary classifier with a unique network architecture designed for detecting OOD samples.

6.1 Setup

In this section, we outline the network architectures employed for training both standard and OOD-sensitive networks. We also detail the ID and OOD datasets used to assess OOD detection performance. Additionally, we describe the metrics chosen to evaluate both ID classification and OOD detection. Lastly, we introduce the implementation details of the proposed CA method.

6.1.1 Network Architectures

We utilize four advanced neural network architectures to train standard networks: ResNet18 [He, Zhang, Ren, and Sun \(2016\)](#), VGG19 [Simonyan and Zisserman \(2015\)](#), SENet [Hu, Shen, and Sun \(2018\)](#), and ViT [Dosovitskiy et al. \(2021\)](#). In addition to these architectures, for training a network sensitive to OOD samples, we also consider two shallow neural network architectures, e.g., Multi-Layer Perceptron (MLP) [Rumelhart, Hinton, and Williams \(1986\)](#) and LeNet [LeCun, Bottou, Bengio, and Haffner \(1998\)](#), and incorporate an Adapt pre-trained Image Model (AIM) into a standard network. Specifically, the utilized MLP is a fully-connected architecture with two hidden layers, each containing 128 ReLU units.

6.1.2 Datasets

We utilize three ID datasets for training our networks: CIFAR10 [Krizhevsky \(2009\)](#), CIFAR100 [Krizhevsky \(2009\)](#), and a mini version of ImageNet [Vinyals, Blundell, Lillicrap, Kavukcuoglu, and Wierstra \(2016\)](#), which contains 100 classes. Specifically, CIFAR10 encompasses 10 classes, while CIFAR100 includes 100 classes. For the evaluation of OOD detection capabilities during testing, we classify the test samples from the ID training datasets as ID. Conversely, samples from seven real-world datasets and two synthesized ones are categorized as OOD.

The real-world OOD datasets are CUB200 [Wah, Branson, Welinder, Perona, and Belongie \(2011\)](#), StanfordDogs120 [Khosla, Jayadevaprakash, Yao, and Fei-Fei \(2011\)](#), OxfordPets37 [Parkhi, Vedaldi, Zisserman, and Jawahar \(2012\)](#), Oxfordflowers102 [Nilsback and Zisserman \(2006\)](#), Caltech256 [Griffin, Holub, and Perona \(2007\)](#), DTD47 [Cimpoi, Maji, Kokkinos, Mohamed, and Vedaldi \(2014\)](#), and COCO [Lin et al. \(2014\)](#). The synthesized OOD samples are drawn from both Gaussian and Uniform distributions [Liang, Li, and Srikant \(2018\)](#). To maintain consistent dimensions across samples, each real-world OOD sample is either resized or cropped to match those of the ID samples. In our evaluation of diverse OOD sample detection capabilities, we present the averaged OOD detection performance over all eight OOD datasets for each method.

6.1.3 Evaluation Metrics

To assess the OOD detection performance, each method assigns an OOD score to every test sample. We utilize the area under the receiver operating characteristic curve (AUROC) [Davis and Goadrich \(2006\)](#) and Detection error [Liang et al. \(2018\)](#) as metrics to gauge the ranking efficacy of these scores. Superior OOD detection is reflected by a higher AUROC and a lower Detection error. Specifically, AUROC evaluates the likelihood that an ID sample receives a score higher than an OOD sample. In contrast, Detection pinpoints the proficiency of a model in recognizing OOD samples, with emphasis on minimizing the misclassification of ID samples as OOD. For assessing ID classification prowess, we employ Accuracy, which denotes the fraction of ID samples the model correctly classifies.

6.1.4 Implementation Details

For the proposed CA algorithm, catering to scenarios with and without training ID data when a standard network is given, we introduce two versions: CA^- and CA^+ . When there is no need to distinguish between CA^- and CA^+ , CA represents both variants. In the absence of training ID data, CA^- employs the regularizer $\mathcal{R}^-(\hat{\mathbf{x}})$ from Eq. (6) during the sample synthesis phase to factor in prior knowledge of the synthesized samples. With training ID data, CA^+ uses the regularizer

$\mathcal{R}^+(\hat{\mathbf{x}})$ from Eq. (5) to align the synthesized samples closer to the training ID data distribution. Unless otherwise mentioned, both CA^- and CA^+ use $a = 1$ in the weight function and $T = 1000$ in the sample synthesis phase. If not specified, both the standard network and its specific binary classifier adopt the same network architecture. For CA^- , parameters are $\beta_{\text{TV}} = 10^{-2}$, $\beta_{l_2} = 3 \cdot 10^{-8}$, and $\beta_f = 1$ for $\mathcal{R}^-(\hat{\mathbf{x}})$. For CA^+ , it is $\beta_{\text{MSE}} = 1$ for $\mathcal{R}^+(\hat{\mathbf{x}})$. Though these parameters produced decent results, the primary emphasis in this paper is not on optimizing the process for synthesis but on leveraging the synthesized samples for an OOD-sensitive binary classifier. Therefore, a comprehensive parameter optimization is beyond the scope of this research.

For a standard network trained on an ID dataset, CA determines the number of random variables, N , based on the count of training ID samples. This implies that the overall synthesized samples amount to $N(T+1)$ for this network. Yet, employing all these synthesized samples is inefficient, leading to suboptimal optimization rates. Moreover, throughout the transfer progression of these synthesized samples, adjacent ones tend to exhibit high similarity. To address this, we strategically select $T' = 6$ samples at uniform intervals from each confidence enhancement procedure, maintaining a temporal gap of $T/(T' - 1)$ between successive samples. Consequently, the aggregate sample count utilized to cultivate an OOD-sensitive binary classifier is NT' .

6.2 Comparison Results

To validate the efficacy of our proposed CA method, we benchmark it against leading OOD detection techniques in scenarios with and without access to training ID data. For a standard network trained using an ID dataset, CA learns its binary classifier to discern between ID and OOD samples under both settings. To ensure fairness, when training ID data is absent, we compare CA^- against renowned OOD detection techniques that do not require retaining or fine-tuning the standard network. These include Maximum over Softmax Probability (MSP) [Hendrycks and Gimpel \(2017\)](#), Energy-based Detector (EBD) [W. Liu et al. \(2020\)](#), GradNorm [R. Huang et al. \(2021\)](#), GEN [X. Liu et al. \(2023\)](#), Decoupling MaxLogit (DML) [Z. Zhang and Xiang \(2023\)](#), ASHD

[et al. \(2023\)](#), and FeatureNorm [Yu et al. \(2023\)](#). Conversely, when training ID data is available, CA^+ is compared to state-of-the-art methods that necessitate retraining the standard network on the ID training data, such as Confidence-Calibrated Classifier (CCC) [Lee et al. \(2018b\)](#), Minimum Others Score (MOS) [R. Huang and Li \(2021\)](#), Density-Driven Regularization (DDR) [W. Huang et al. \(2022\)](#), Watermarking [Wang et al. \(2022\)](#), CIDER [Ming et al. \(2023\)](#), HEAT [Lafon et al. \(2023\)](#), and Dual Representation Learning (DRL) [Zhao and Cao \(2023\)](#).

6.2.1 Methods without Training ID Data

As depicted in Table 1, CA^- exhibits exceptional OOD detection performance, especially compared to methods without training ID data access. Across three renowned datasets and four distinct neural architectures, CA^- consistently set the benchmark. On CIFAR10 using ResNet18, CA not only attains an unmatched AUROC of 86.5%, outpacing its closest contender by 1.3%, but also registers the most competitive Detection score at 18.2%. When assessed on CIFAR100, it marks an AUROC of 88.3%, leading the runner-up by 0.7%, and delivers a Detection score of 17.2%. Moreover, on ImageNet, CA showcases a remarkable 81.6% AUROC, a distinct lead of 0.9% over the next best, coupled with the leading Detection score of 22.8%. The consistent performance of the CA^- algorithm stems from its adeptness in synthesizing ID and OOD samples. These samples proficiently probe the inherent distribution vulnerabilities of standard networks, especially pinpointing samples with high-confidence predictions. Consequently, the binary classifier exhibits heightened sensitivity towards OOD samples, accentuating the confidence disparity between ID and OOD samples by penalizing the latter.

6.2.2 Methods with Training ID Data

The OOD detection performance, for methods having access to training ID data, is depicted in Table 2. CA^+ demonstrates unparalleled excellence, surpassing other OOD detection methods across every dataset and architecture. On CIFAR10 with ResNet18, CA^+ achieves an exceptional AUROC of 88.8%, outperforming the next best, HEAT, by 3.7%. This dominance extends

Table 1 Performance comparison among OOD detection methods without access to training ID data. ‘A’ and ‘D’ represents the metrics AUROC and Detection Error, respectively. A higher AUROC and a lower Detection value represent superior performance. Results are averaged over five random trials for each method, with the best results highlighted in bold.

| ID | Methods | ResNet18 | | VGG19 | | SENet | | ViT | |
|----------|-----------------|--------------|----------------|--------------|----------------|--------------|----------------|--------------|----------------|
| | | A \uparrow | D \downarrow | A \uparrow | D \downarrow | A \uparrow | D \downarrow | A \uparrow | D \downarrow |
| CIFAR10 | MSP | 77.2 | 26.0 | 73.0 | 29.1 | 78.4 | 25.8 | 76.1 | 26.8 |
| | EBD | 77.9 | 25.2 | 73.9 | 28.1 | 79.1 | 25.6 | 76.3 | 26.4 |
| | GradNorm | 78.6 | 24.1 | 75.6 | 27.1 | 81.9 | 21.6 | 80.0 | 24.4 |
| | GEN | 80.7 | 24.3 | 78.4 | 25.8 | 87.3 | 18.5 | 82.9 | 22.0 |
| | DML | 82.4 | 21.8 | 78.1 | 24.4 | 82.8 | 22.4 | 80.8 | 22.5 |
| | ASH | 84.4 | 19.5 | 80.5 | 22.9 | 84.7 | 20.6 | 83.3 | 21.2 |
| | FeatureNorm | 85.2 | 19.7 | 76.6 | 25.9 | 85.3 | 20.1 | 84.4 | 19.5 |
| | CA ⁻ | 86.5 | 18.2 | 83.1 | 21.8 | 88.4 | 16.9 | 85.3 | 17.9 |
| CIFAR100 | MSP | 78.3 | 27.6 | 73.6 | 31.1 | 77.3 | 28.5 | 78.5 | 27.3 |
| | EBD | 80.3 | 27.0 | 74.5 | 30.7 | 79.8 | 25.7 | 80.0 | 25.9 |
| | GradNorm | 83.4 | 23.3 | 77.9 | 27.2 | 83.7 | 21.2 | 81.7 | 25.9 |
| | GEN | 87.2 | 17.6 | 80.9 | 24.4 | 86.3 | 19.3 | 85.1 | 20.6 |
| | DML | 83.8 | 21.5 | 83.8 | 20.8 | 89.0 | 17.2 | 84.0 | 22.5 |
| | ASH | 84.9 | 20.9 | 85.0 | 19.1 | 84.7 | 22.3 | 83.3 | 22.4 |
| | FeatureNorm | 87.6 | 17.4 | 83.3 | 23.4 | 84.4 | 22.0 | 86.7 | 20.1 |
| | CA ⁻ | 88.3 | 17.2 | 86.2 | 19.5 | 90.1 | 15.9 | 87.6 | 18.5 |
| ImageNet | MSP | 70.7 | 30.6 | 68.8 | 34.2 | 65.7 | 37.5 | 75.5 | 26.1 |
| | EBD | 72.2 | 29.6 | 69.8 | 32.9 | 66.5 | 37.2 | 76.3 | 26.0 |
| | GradNorm | 73.4 | 29.1 | 75.2 | 26.4 | 70.2 | 32.9 | 79.2 | 23.1 |
| | GEN | 80.7 | 23.4 | 76.4 | 26.0 | 74.0 | 30.0 | 84.2 | 20.3 |
| | DML | 76.7 | 26.4 | 76.4 | 25.7 | 76.8 | 27.7 | 82.8 | 19.8 |
| | ASH | 78.1 | 25.8 | 77.9 | 24.9 | 76.9 | 27.3 | 82.4 | 20.0 |
| | FeatureNorm | 79.1 | 24.3 | 78.8 | 24.3 | 77.1 | 28.3 | 82.3 | 19.2 |
| | CA ⁻ | 81.6 | 22.8 | 79.4 | 23.8 | 78.1 | 26.3 | 84.5 | 18.7 |

to VGG19 with an AUROC of 85.2%, outpacing Watermarking by 2.9%, and to SENet with an impressive 90.4% AUROC, leading HEAT by 0.7%. On ViT, its AUROC stands at 88.5%, besting DRL by 3.5%. CIFAR100 echoes the trends observed in CIFAR10. For ImageNet, while CA⁺ and Watermarking share comparable AUROCs on ResNet18, CA⁺ exhibits a slight edge in the Detection metric. The AUROC achieved by CA⁺ on VGG19 is 82.4%, outstripping CIDER by 2.4%, and on SENet, it peaks at 83.6%, surpassing DRL by 3.2%. On ViT, the algorithm attains an 86.5% AUROC, edging out Watermarking by 0.4%. Clearly, CA⁺ sets the benchmark in OOD detection across various datasets and architectures. This can be attributed to the sample synthesis phase of CA⁺ which adeptly synthesizes specific OOD samples. The accompanying binary

classifier fortifies OOD sensitivity by fostering low-confidence predictions for these samples.

6.3 Parameter Analysis

In this section, we explore the influence of the maximum number of iterations T for synthesizing samples and the weight function coefficient a for adjusting predicted label distributions. The network architecture utilized is ResNet18, and the standard network is trained on the CIFAR10 ID dataset.

6.3.1 Maximum Transition Time

To understand the effect of the maximum transition time T in the sample synthesis phase, we select it from $\{100, 500, 1000, 1500, 2000\}$, and the results are presented in Fig. 4. CA⁺ consistently

Table 2 Performance comparison among OOD detection methods with access to training ID data. ‘A’ and ‘D’ represents the metrics AUROC and Detection Error, respectively. A higher AUROC and a lower Detection value represent superior performance. Results are averaged over five random trials for each method, with the best results highlighted in bold.

| ID | Methods | ResNet18 | | VGG19 | | SENet | | ViT | |
|----------|-----------------|--------------|----------------|--------------|----------------|--------------|----------------|--------------|----------------|
| | | A \uparrow | D \downarrow | A \uparrow | D \downarrow | A \uparrow | D \downarrow | A \uparrow | D \downarrow |
| CIFAR10 | CCC | 76.4 | 29.3 | 72.6 | 33.6 | 77.2 | 28.4 | 78.6 | 25.6 |
| | MOS | 78.8 | 27.1 | 73.7 | 32.1 | 80.5 | 25.5 | 80.6 | 23.2 |
| | DDR | 85.2 | 17.2 | 80.7 | 25.0 | 86.8 | 18.3 | 83.6 | 19.1 |
| | Watermarking | 83.3 | 20.9 | 82.3 | 21.6 | 87.6 | 17.3 | 81.3 | 24.2 |
| | CIDER | 87.1 | 16.4 | 75.7 | 29.2 | 84.2 | 19.7 | 83.9 | 21.2 |
| | HEAT | 87.8 | 17.6 | 82.2 | 23.4 | 89.7 | 17.4 | 84.4 | 20.3 |
| | DRL | 83.3 | 20.9 | 75.7 | 29.2 | 82.3 | 22.0 | 85.0 | 18.3 |
| | CA ⁺ | 88.8 | 16.0 | 85.2 | 20.1 | 90.4 | 14.3 | 88.5 | 17.4 |
| CIFAR100 | CCC | 76.4 | 29.3 | 72.6 | 33.6 | 77.2 | 28.4 | 78.6 | 25.6 |
| | MOS | 78.8 | 27.1 | 73.7 | 32.1 | 80.5 | 25.5 | 80.6 | 23.2 |
| | DDR | 85.2 | 17.2 | 80.7 | 25.0 | 86.8 | 18.3 | 83.6 | 19.1 |
| | Watermarking | 83.3 | 20.9 | 82.3 | 21.6 | 87.6 | 17.3 | 81.3 | 24.2 |
| | CIDER | 87.1 | 16.4 | 75.7 | 29.2 | 84.2 | 19.7 | 83.9 | 21.2 |
| | HEAT | 87.8 | 17.6 | 82.2 | 23.4 | 89.7 | 17.4 | 84.4 | 20.3 |
| | DRL | 83.3 | 20.9 | 75.7 | 29.2 | 82.3 | 22.0 | 85.0 | 18.3 |
| | CA ⁺ | 88.8 | 16.0 | 85.2 | 20.1 | 90.4 | 14.3 | 88.5 | 17.4 |
| ImageNet | CCC | 74.6 | 29.0 | 69.4 | 32.2 | 67.8 | 35.4 | 76.9 | 25.3 |
| | MOS | 77.3 | 27.6 | 77.2 | 25.6 | 80.4 | 25.1 | 83.3 | 19.4 |
| | DDR | 82.5 | 24.8 | 75.9 | 24.2 | 74.6 | 28.4 | 82.5 | 21.6 |
| | Watermarking | 85.0 | 24.0 | 76.6 | 25.4 | 77.7 | 27.6 | 86.1 | 17.7 |
| | CIDER | 83.5 | 23.7 | 80.1 | 21.4 | 73.4 | 28.6 | 77.9 | 25.4 |
| | HEAT | 79.0 | 25.8 | 70.6 | 32.0 | 74.4 | 29.7 | 84.4 | 19.6 |
| | DRL | 84.5 | 24.6 | 78.0 | 25.1 | 80.4 | 25.1 | 82.2 | 21.0 |
| | CA ⁺ | 85.2 | 23.6 | 82.4 | 20.1 | 83.6 | 21.2 | 86.5 | 16.8 |

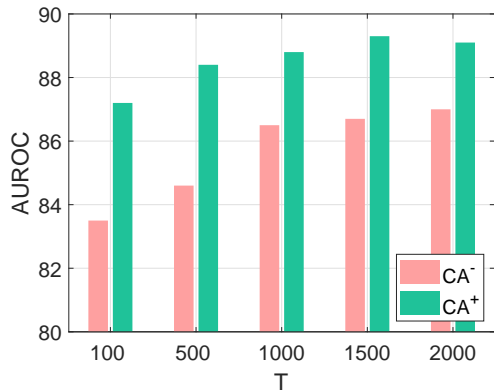


Fig. 4 OOD detection performance comparison of CA⁻ and CA⁺ over varying maximum transition time T .

achieves a higher AUROC compared to CA⁻,

suggesting superior performance, and the performance for both methods improves as the maximum transition time increases. This is because, during the sample synthesis phase, OOD samples gradually transform into ID samples. By incorporating real ID samples and increasing the maximum transition time, the synthesized samples at the end are brought closer to the distribution of real ID samples. Thus, the OOD samples evolve towards the ID in a more accurate direction, and this binary classifier can leverage these more accurate samples to learn to differentiate between the two types of samples.

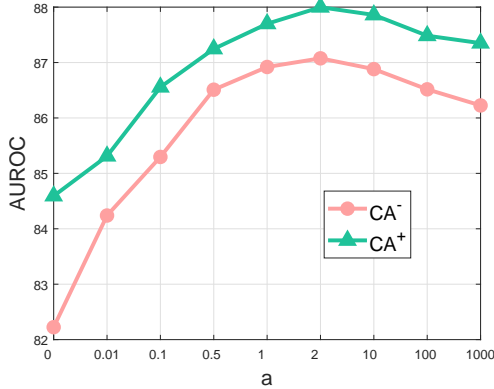


Fig. 5 OOD detection performance comparison of CA⁻ and CA⁺ over varying weight function coefficient a .

6.3.2 Weight Function Coefficient

To understand the effect of the weight function coefficient a in adjusting predicted label distributions, we select it from $\{100, 500, 1000, 1500, 2000\}$, and the results are presented in Fig. 5. We observe that CA⁺ method consistently outperforms the CA⁻ method across the entire range of a values, and both methods experience a peak in their performance, with CA⁺ reaching a higher peak value in terms of AUROC. Specifically, the performance of CA⁺ peaks at an AUROC value around a value of 1, after which it starts to slightly decline but remains above CA⁻ throughout. Conversely, the performance of CA⁻ sees a steady increase and eventually declines as a approaches 1000. The experimental results are largely consistent with the theoretical insights provided by Corollary 1, indicating that a larger value of a results in better differentiation between ID and OOD samples. While Corollary 1 suggests that the effect increases with the value of a , the experimental data shows that once a reaches a certain threshold, such as 1, the performance slightly decreases with further increases in a . This can be understood from Eq. (19), we can deduce that when a is large, the gradient of the weight function becomes small. Moreover, a very large a will result in most of the synthesized samples being treated as OOD, leading to a class imbalance issue. Thus, in practice, while a large a can lead to differentiated results, an overly large value might slightly compromise the outcomes.

When $a = 0$, the CR method simply transfers the knowledge extracted from the standard

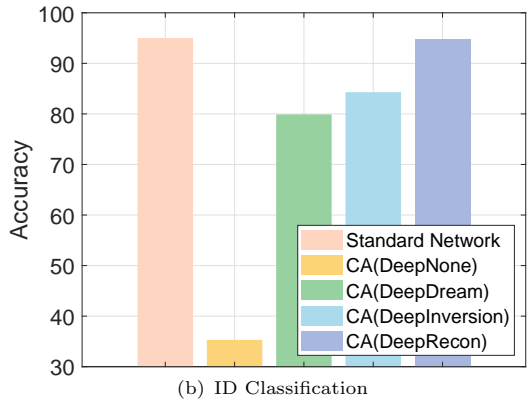
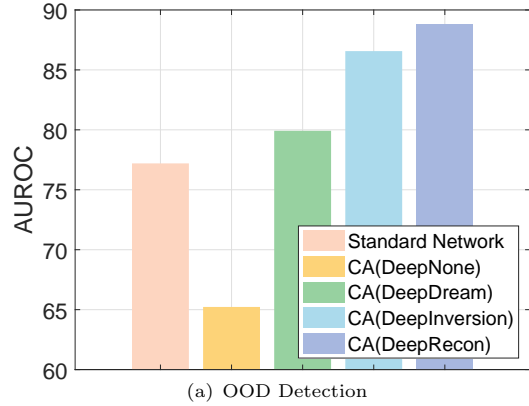


Fig. 6 Comparison of OOD Detection and ID Classification performances across various CA method variants and the standard network. Best viewed in color.

network directly into the binary classifier. However, when $a > 0$, the confidence of the network is adjusted according to Eq. (9). We observe that the performance is significantly better when $a > 0$, indicating that CR should go beyond just a brief transfer of knowledge. Instead, it should refine the knowledge to further enhance the sensitivity to OOD samples.

6.4 Regularizer Analysis

For the parameterized Markov chain described in Eq. (7), different regularizers, $\mathcal{R}(\hat{\mathbf{x}})$, can shape the ID samples synthesized from OOD inputs. We evaluate the variants of our proposed CA method with distinct regularizers. Setting the OOD detection and ID classification of the standard network as our benchmarks, we contrast each CA variant against these standards using AUROC and Accuracy metrics. Without access to training ID data, we explore three

Table 3 Performance evaluation of OOD detection and ID classification for CA^- and CA^+ using various binary classifier architectures.

| Method | Metric | Deep | | | | Shallow | | Adapter |
|--------|----------|-------------|-------|-------------|-------------|---------|-------|-------------|
| | | ResNet18 | VGG19 | SENet | ViT | MLP | LeNet | AIM |
| CA^- | AUROC | 86.6 | 56.5 | 84.2 | 77.3 | 66.3 | 64.5 | 76.3 |
| | Accuracy | 92.7 | 72.4 | 84.9 | 82.9 | 18.0 | 32.2 | 95.0 |
| CA^+ | AUROC | 88.8 | 88.4 | 89.2 | 86.8 | 73.7 | 84.2 | 85.9 |
| | Accuracy | 94.8 | 93.7 | 94.8 | 95.4 | 56.9 | 73.0 | 94.9 |

CA versions: CA(DeepNone), CA(DeepDream), and CA(DeepInversion). CA(DeepNone) evolves OOD samples into ID without constraints, optimizing only for cross-entropy loss with random labels. CA(DeepInversion), or CA^- , applies $\mathcal{R}^-(\hat{\mathbf{x}})$ to integrate ID sample prior knowledge, while CA(DeepDream) is a specialized CA(DeepInversion) version with $\beta_f = 0$. With access to ID data, we use $\mathcal{R}^+(\hat{\mathbf{x}})$ to align synthesized and original sample distributions, creating the CA variant named CA(DeepRecon) or CA^+ . Specifically, we utilize the trained backbone of the OOD-sensitive binary classifier to classify ID samples.

We evaluate the OOD detection and ID classification performances of various CA method variants, alongside the benchmark standard network, using ResNet18 trained on CIFAR10. The results are depicted in Fig. 6. Fig. 6(a) shows that while some CA variants outperform the standard network in detecting OOD samples, CA(DeepNone) trails behind. This underperformance of CA(DeepNone) arises because it does not incorporate any constraints for the synthesized samples, suggesting that by the end of the transition chain, these samples are highly likely to be OOD with pronounced confidence. As a result, there are insufficient ID samples to train the binary classifier to differentiate between ID and OOD samples. Conversely, Fig. 6(b) highlights a performance disparity among the methods in classifying ID samples. All CA variants display limited classification accuracy. This is anticipated, as the CA variants primarily aim to enhance OOD sensitivity through training on synthesized ID and OOD samples, rather than improving generalization for predicting ID labels. Importantly, the backbone of a binary classifier maintains some capability for ID classification. This arises from

our approach of using an auxiliary network during the knowledge distillation from the standard network to the binary classifier, designed to emulate the output of the standard network to retain its intrinsic knowledge. The binary classifier is then built upon this output. Furthermore, the aptitude of the network to classify ID samples invariably impacts its OOD detection prowess. A more competent network in discerning ID samples will be adept at spotting nuanced differences between ID and OOD samples, ensuring precise OOD detection.

6.5 Transferability Analysis

We assess the adaptability of synthesized samples using a standard network, particularly a ResNet18 trained on the CIFAR10 dataset. To achieve this, we utilize these synthesized samples to instruct various binary classifiers, each characterized by unique network architectures. They are primarily grouped into deep neural networks (such as ResNet18 He et al. (2016), VGG19 Simonyan and Zisserman (2015), SENet Hu et al. (2018), and ViT Dosovitskiy et al. (2021)), shallow neural networks (like MLP Rumelhart et al. (1986) and LeNet LeCun et al. (1998)), and the adapter model AIM T. Yang et al. (2023), which is particularly constructed on the base of the standard network.

Performance results are comprehensively detailed in Table 3. Among the deep neural network category, ResNet18 exhibits prominent results, especially in conjunction with CA^+ . The outcomes highlight that shallow networks, primarily MLP, lag behind their deeper analogs in efficiency. The AIM, conceived as an adapter model, showcases competitive outcomes. In general, certain architectures yield remarkable performance, suggesting that the synthesized

samples from a standard network can adeptly train a binary classifier sensitive to OOD across varying network architectures. Additionally, when the standard network and the binary classifier possess identical architecture, there is a marked enhancement in performance. This can be attributed to the consistent feature extraction offered by the uniform network structure. While diverse architectures may introduce variations in the feature distributions of the produced samples, a shared architecture ensures that the feature space remains aligned and consistent, bolstering the generalization ability of the binary classifier in distinguishing between ID and OOD samples.

7 Conclusions and Future Work

In this study, we introduced an innovative learning paradigm, named OOD knowledge distillation, designed to enhance the sensitivity of deep neural networks towards OOD samples by training a specialized binary classifier adept at differentiating between ID and OOD samples. Confidence Amendment (CA) method is a pivotal element of this framework. A key aspect of CA is the structured transition of an OOD sample towards an ID counterpart, emphasizing the incremental establishment of trust in its prediction confidence. These synthesized samples with adjusted predicted label distributions are utilized to train an OOD-sensitive binary classifier. From a theoretical standpoint, the generalization error bound underscores the capability of the classifier in managing unfamiliar ID and OOD samples when paired with a suitable weight function. Comprehensive experiments on various datasets and architectures validate the effectiveness of our method. A promising avenue for future research involves exploring methods that can further transform training ID samples into network-tailored OOD samples to enhance the OOD sensitivity of neural networks.

Acknowledgments. This work was supported in part by the Australian Research Council Discovery under Grant DP190101079 and in part by the Future Fellowship under Grant FT190100734.

Declarations

Data Availability

The datasets analysed during the current study are available in CIFAR10 (<https://www.cs.toronto.edu/~kriz/cifar.html>), CIFAR100 (<https://www.cs.toronto.edu/~kriz/cifar.html>), ImageNet (<https://github.com/yaoyao-liu/mini-imagenet-tools>), CUB200 (https://www.vision.caltech.edu/datasets/cub_200_2011/), Stanford-Dogs120 (<http://vision.stanford.edu/aditya86/ImageNetDogs/>), OxfordPets37 (<https://www.robots.ox.ac.uk/~vgg/data/pets/>), Oxford-flowers102 (<https://www.robots.ox.ac.uk/~vgg/data/flowers/>), Caltech256 (<https://www.kaggle.com/jessicali9530/caltech256>), DTD47 (<https://www.robots.ox.ac.uk/~vgg/data/dtd/>) and COCO (<https://cocodataset.org/>).

References

- Ahn, Y.H., Park, G., Kim, S.T. (2023). Line: Out-of-distribution detection by leveraging important neurons. *Proceedings of the IEEE/CVF conference on computer vision and pattern recognition* (pp. 19852–19862).
- Allen-Zhu, Z., & Li, Y. (2023). Towards understanding ensemble, knowledge distillation and self-distillation in deep learning. *11th international conference on learning representations* (pp. 1–13).
- Bartlett, P., & Shawe-Taylor, J. (1999). Generalization performance of support vector machines and other pattern classifiers. *Advances in Kernel methods—support vector learning*, 43–54,
- Bibas, K., Feder, M., Hassner, T. (2021). Single layer predictive normalized maximum likelihood for out-of-distribution detection. *Advances in neural information processing systems 34* (pp. 1179–1191).
- Cao, S., & Zhang, Z. (2022). Deep hybrid models for out-of-distribution detection. *Proceedings of the IEEE/CVF conference on computer vision and pattern recognition* (pp. 4723–4733).

- Chen, H., Wang, Y., Xu, C., Yang, Z., Liu, C., Shi, B., ... Tian, Q. (2019). Data-free learning of student networks. *IEEE/CVF international conference on computer vision* (pp. 3513–3521).
- Cimpoi, M., Maji, S., Kokkinos, I., Mohamed, S., Vedaldi, A. (2014). Describing textures in the wild. *Proceedings of the IEEE/CVF conference on computer vision and pattern recognition* (pp. 3606–3613).
- Davis, J., & Goadrich, M. (2006). The relationship between precision-recall and roc curves. *International conference on machine learning* (pp. 233–240).
- Djurisic, A., Bozanic, N., Ashok, A., Liu, R. (2023). Extremely simple activation shaping for out-of-distribution detection. *11th international conference on learning representations* (pp. 1–22).
- Dong, X., Guo, J., Li, A., Ting, W., Liu, C., Kung, H.T. (2022). Neural mean discrepancy for efficient out-of-distribution detection. *Proceedings of the IEEE/CVF conference on computer vision and pattern recognition* (pp. 19195–19205).
- Dosovitskiy, A., Beyer, L., Kolesnikov, A., Weissenborn, D., Zhai, X., Unterthiner, T., ... Houlsby, N. (2021). An image is worth 16x16 words: Transformers for image recognition at scale. *9th international conference on learning representations* (pp. 1–21).
- Duan, Y., Wang, M., Wen, Z., Yuan, Y. (2020). Adaptive low-nonnegative-rank approximation for state aggregation of markov chains. *SIAM J. Matrix Anal. Appl.*, 41(1), 244–278,
- Gal, Y., & Ghahramani, Z. (2016). Dropout as a bayesian approximation: Representing model uncertainty in deep learning. *International conference on machine learning* (Vol. 48, pp. 1050–1059).
- Gomes, E.D.C., Alberge, F., Duhamel, P., Piantanida, P. (2022). IGEOOD: an information geometry approach to out-of-distribution detection. *10th international conference on learning representations* (pp. 1–37).
- Goodfellow, I.J., Pouget-Abadie, J., Mirza, M., Xu, B., Warde-Farley, D., Ozair, S., ... Bengio, Y. (2014). Generative adversarial nets. *Advances in neural information processing systems 27* (pp. 2672–2680).
- Goodfellow, I.J., Shlens, J., Szegedy, C. (2015). Explaining and harnessing adversarial examples. *3rd international conference on learning representations* (pp. 1–11).
- Gou, J., Yu, B., Maybank, S.J., Tao, D. (2021). Knowledge distillation: A survey. *Int. J. Comput. Vis.*, 129(6), 1789–1819,
- Griffin, G., Holub, A., Perona, P. (2007). *Caltech-256 object category dataset* (Tech. Rep.).
- He, K., Zhang, X., Ren, S., Sun, J. (2016). Deep residual learning for image recognition. *Proceedings of the IEEE/CVF conference on computer vision and pattern recognition* (pp. 770–778).
- Hein, M., Andriushchenko, M., Bitterwolf, J. (2019). Why relu networks yield high-confidence predictions far away from the training data and how to mitigate the problem. *Proceedings of the IEEE/CVF conference on computer vision and pattern recognition* (pp. 41–50).
- Hendrycks, D., Basart, S., Mazeika, M., Zou, A., Kwon, J., Mostajabi, M., ... Song, D. (2022). Scaling out-of-distribution detection for real-world settings. *International conference on machine learning* (pp. 8759–8773).
- Hendrycks, D., & Gimpel, K. (2017). A baseline for detecting misclassified and out-of-distribution examples in neural networks. *5th international conference on learning representations, ICLR 2017, toulon, france, april 24-26, 2017, conference track proceedings* (pp. 1–12).

- Heo, B., Lee, M., Yun, S., Choi, J.Y. (2019). Knowledge distillation with adversarial samples supporting decision boundary. *The thirty-third AAAI conference on artificial intelligence* (pp. 3771–3778).
- Hinton, G.E., Vinyals, O., Dean, J. (2015). Distilling the knowledge in a neural network. *CoRR*, 1–9,
- Ho, J., Jain, A., Abbeel, P. (2020). Denoising diffusion probabilistic models. *Advances in neural information processing systems 33* (pp. 1–25).
- Hsu, Y., Shen, Y., Jin, H., Kira, Z. (2020). Generalized ODIN: detecting out-of-distribution image without learning from out-of-distribution data. *Proceedings of the IEEE/CVF conference on computer vision and pattern recognition* (pp. 10948–10957).
- Hu, J., Shen, L., Sun, G. (2018). Squeeze-and-excitation networks. *Proceedings of the IEEE/CVF conference on computer vision and pattern recognition* (pp. 7132–7141).
- Huang, R., Geng, A., Li, Y. (2021). On the importance of gradients for detecting distributional shifts in the wild. *Advances in neural information processing systems 34* (pp. 677–689).
- Huang, R., & Li, Y. (2021). MOS: Towards scaling out-of-distribution detection for large semantic space. *Proceedings of the IEEE/CVF conference on computer vision and pattern recognition* (pp. 8710–8719).
- Huang, W., Wang, H., Xia, J., Wang, C., Zhang, J. (2022). Density-driven regularization for out-of-distribution detection. *Advances in neural information processing systems 36* (pp. 1–14).
- Kearns, M.J., & Schapire, R.E. (1994). Efficient distribution-free learning of probabilistic concepts. *J. Comput. Syst. Sci.*, 48(3), 464–497,
- Khosla, A., Jayadevaprakash, N., Yao, B., Fei-Fei, L. (2011). Novel dataset for fine-grained image categorization. *Proc. cvpr workshop on fine-grained visual categorization* (pp. 1–2).
- Kingma, D.P., & Welling, M. (2014). Auto-encoding variational bayes. *2nd international conference on learning representations* (pp. 1–14).
- Krizhevsky, A. (2009). *Learning multiple layers of features from tiny images* (Tech. Rep.).
- Lafon, M., Ramzi, E., Rambour, C., Thome, N. (2023). Hybrid energy based model in the feature space for out-of-distribution detection. *International conference on machine learning* (Vol. 202, pp. 18250–18268).
- LeCun, Y., Bottou, L., Bengio, Y., Haffner, P. (1998). Gradient-based learning applied to document recognition. *Proc. IEEE*, 86(11), 2278–2324,
- Lee, K., Lee, H., Lee, K., Shin, J. (2018b). Training confidence-calibrated classifiers for detecting out-of-distribution samples. *6th international conference on learning representations* (pp. 1–16).
- Lee, K., Lee, K., Lee, H., Shin, J. (2018a). A simple unified framework for detecting out-of-distribution samples and adversarial attacks. *Advances in neural information processing systems 31* (pp. 7167–7177).
- Liang, S., Li, Y., Srikant, R. (2018). Enhancing the reliability of out-of-distribution image detection in neural networks. *6th international conference on learning representations* (pp. 1–27).
- Lin, T., Maire, M., Belongie, S.J., Hays, J., Perona, P., Ramanan, D., ... Zitnick, C.L. (2014). Microsoft COCO: Common objects in context. *Proceedings of the european conference on computer vision* (Vol. 8693, pp. 740–755).

- Liu, W., Wang, X., Owens, J.D., Li, Y. (2020). Energy-based out-of-distribution detection. *Advances in neural information processing systems 33* (pp. 1–13).
- Liu, X., Lochman, Y., Zach, C. (2023). GEN: pushing the limits of softmax-based out-of-distribution detection. *Proceedings of the IEEE/CVF conference on computer vision and pattern recognition* (pp. 23946–23955).
- Lopes, R.G., Fenu, S., Starner, T. (2017). Data-free knowledge distillation for deep neural networks. *CoRR*, 1–8,
- Lopez-Paz, D., Bottou, L., Schölkopf, B., Vapnik, V. (2016). Unifying distillation and privileged information. *4th international conference on learning representations* (pp. 1–10).
- Ming, Y., Sun, Y., Dia, O., Li, Y. (2023). How to exploit hyperspherical embeddings for out-of-distribution detection? *11th international conference on learning representations* (pp. 1–19).
- Mordvintsev, A., Olah, C., Tyka, M. (2015). *Inceptionism: Going deeper into neural networks*. Google Research Blog.
- Nilsback, M., & Zisserman, A. (2006). A visual vocabulary for flower classification. *IEEE computer society conference on computer vision and pattern* (pp. 1447–1454).
- Olber, B., Radlak, K., Popowicz, A., Szczepankiewicz, M., Chachula, K. (2023). Detection of out-of-distribution samples using binary neuron activation patterns. *Proceedings of the IEEE/CVF conference on computer vision and pattern recognition* (pp. 3378–3387).
- Parkhi, O.M., Vedaldi, A., Zisserman, A., Jawahar, C.V. (2012). Cats and dogs. *Proceedings of the IEEE/CVF conference on computer vision and pattern recognition* (pp. 3498–3505).
- Romero, A., Ballas, N., Kahou, S.E., Chassang, A., Gatta, C., Bengio, Y. (2015). Fitnets: Hints for thin deep nets. *3rd international conference on learning representations* (pp. 1–13).
- Rumelhart, D.E., Hinton, G.E., Williams, R.J. (1986). Learning representations by back-propagating errors. *Nature*, 323(6088), 533–536,
- Salehi, M., Mirzaei, H., Hendrycks, D., Li, Y., Rohban, M.H., Sabokrou, M. (2022). A unified survey on anomaly, novelty, open-set, and out of-distribution detection: Solutions and future challenges. *Trans. Mach. Learn. Res.*, 2022, 1–81,
- Shalev-Shwartz, S., & Ben-David, S. (2014). *Understanding machine learning from theory to algorithms*. Cambridge University Press.
- Shawe-Taylor, J., Bartlett, P.L., Williamson, R.C., Anthony, M. (1998). Structural risk minimization over data-dependent hierarchies. *IEEE Trans. Inf. Theory*, 44(5), 1926–1940,
- Simonyan, K., & Zisserman, A. (2015). Very deep convolutional networks for large-scale image recognition. *3rd international conference on learning representations* (pp. 1–14).
- Sohl-Dickstein, J., Weiss, E.A., Maheswaranathan, N., Ganguli, S. (2015). Deep unsupervised learning using nonequilibrium thermodynamics. *International conference on machine learning* (Vol. 37, pp. 2256–2265).
- Sun, Y., Guo, C., Li, Y. (2021). ReAct: out-of-distribution detection with rectified activations. *Advances in neural information processing systems 34* (pp. 144–157).
- Suzuki, T., Abe, H., Nishimura, T. (2020). Compression based bound for non-compressed

- network: unified generalization error analysis of large compressible deep neural network. *8th international conference on learning representations* (pp. 1–34).
- Vapnik, V. (2006). *Estimation of dependences based on empirical data*. Springer Science & Business Media.
- Vapnik, V.N., & Chervonenkis, A.Y. (2015). On the uniform convergence of relative frequencies of events to their probabilities. *Measures of complexity: festschrift for alexey chervonenkis* (pp. 11–30). Springer.
- Vinyals, O., Blundell, C., Lillicrap, T., Kavukcuoglu, K., Wierstra, D. (2016). Matching networks for one shot learning. *Advances in neural information processing systems 29* (pp. 3630–3638).
- Wah, C., Branson, S., Welinder, P., Perona, P., Belongie, S. (2011). *The Caltech-UCSD birds-200-2011 dataset* (Tech. Rep.).
- Wang, Q., Liu, F., Zhang, Y., Zhang, J., Gong, C., Liu, T., Han, B. (2022). Watermarking for out-of-distribution detection. *Advances in neural information processing systems 36* (pp. 1–13).
- Yang, J., Wang, P., Zou, D., Zhou, Z., Ding, K., Peng, W., ... Liu, Z. (2022). Openood: Benchmarking generalized out-of-distribution detection. *Advances in neural information processing systems 36* (pp. 1–14).
- Yang, J., Zhou, K., Li, Y., Liu, Z. (2021). Generalized out-of-distribution detection: A survey. *CoRR*, 1–20,
- Yang, J., Zhou, K., Liu, Z. (2023). Full-spectrum out-of-distribution detection. *Int. J. Comput. Vis.*, 131(10), 2607–2622,
- Yang, T., Zhu, Y., Xie, Y., Zhang, A., Chen, C., Li, M. (2023). AIM: adapting image models for efficient video action recognition. *11th international conference on learning representations* (pp. 1–18).
- Yin, H., Molchanov, P., Álvarez, J.M., Li, Z., Mallya, A., Hoiem, D., ... Kautz, J. (2020). Dreaming to distill: Data-free knowledge transfer via deepinversion. *Proceedings of the IEEE/CVF conference on computer vision and pattern recognition* (pp. 8712–8721).
- Yu, Y., Shin, S., Lee, S., Jun, C., Lee, K. (2023). Block selection method for using feature norm in out-of-distribution detection. *Proceedings of the IEEE/CVF conference on computer vision and pattern recognition* (pp. 15701–15711).
- Zhang, J., Fu, Q., Chen, X., Du, L., Li, Z., Wang, G., ... Zhang, D. (2023). Out-of-distribution detection based on in-distribution data patterns memorization with modern hopfield energy. *11th international conference on learning representations* (pp. 1–19).
- Zhang, Z., & Xiang, X. (2023). Decoupling maxlogit for out-of-distribution detection. *Proceedings of the IEEE/CVF conference on computer vision and pattern recognition* (pp. 3388–3397).
- Zhao, Z., & Cao, L. (2023). Dual representation learning for out-of-distribution detection. *Trans. Mach. Learn. Res.*, 2023, 1–21,
- Zhao, Z., Cao, L., Lin, K. (2023a). Out-of-distribution detection by cross-class vicinity distribution of in-distribution data. *IEEE Trans. Neural Networks Learn. Syst.*, 1-12,
- Zhao, Z., Cao, L., Lin, K. (2023b). Revealing the distributional vulnerability of discriminators by implicit generators. *IEEE Trans. Pattern Anal. Mach. Intell.*, 45(7), 8888–8901,
- Zhao, Z., Cao, L., Lin, K.-Y. (2023c). Supervision adaptation balancing in-distribution generalization and out-of-distribution detection. *IEEE Trans. Pattern Anal. Mach. Intell.*, 1-16,

- Zhu, J., Li, H., Yao, J., Liu, T., Xu, J., Han, B. (2023). Unleashing mask: Explore the intrinsic out-of-distribution detection capability. *International conference on machine learning* (pp. 43068–43104).
- Zhu, Y., Chen, Y., Xie, C., Li, X., Zhang, R., Xue, H., ... Chen, Y. (2022). Boosting out-of-distribution detection with typical features. *Advances in neural information processing systems 36* (pp. 1–12).